Ecological Indicators 154 (2023) 110555

Contents lists available at ScienceDirect

Ecological Indicators

journal homepage: www.elsevier.com/locate/ecolind

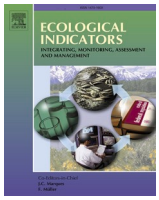

Declining trees growth and vegetation productivity resulting from decreasing soil water contents induced by tunnels excavation in karst mountain areas

Sibo Zeng, Yongjun Jiang *, Ze Wu, Caiyun Zhang, Tongru Lv

Chongqing Key Laboratory of Karst Environment & School of Geographical Sciences of Southwest University, Chongqing 400715, China

ARTICLE INFO

Keywords:
NDVI
NPP
Plant growth
Soil water storage
Tunnel excavation
Tree-ring data

ABSTRACT

Tunnel construction in karst areas greatly impacts the local hydrological conditions. The drawdown of groundwater levels and the loss of soil water storage due to tunneling limit the available water resources on the karst land surface, and this may affect the function of plants. Here, we evaluated the responses of the radial growth rates of two major tree species (Masson pine and Camphor laurel) to a tunneling induced water stress event in a typical karst trough valley. Meanwhile, to discuss the overall influence of tunnel excavation on plant growth in all vegetation cover types, the dynamics of vegetation productivity around the tunnel were evaluated using remote sensing indices, the Normalized Difference Vegetation Index (NDVI), and Net Primary Productivity (NPP). Furthermore, we estimated the spatial–temporal variations of NDVI and NPP in other tunneling regions of Southwest China. The results showed that the soil moisture contents (SMC) around the Zhongliang Mountain Railway Line 6 (ZMRL6) tunnel had dramatically declined −5.06%~−10.53% within the areas < 1500 m. After the excavation of ZMRL6 tunnel, the basal area increment (BAI) for the tree-ring widths of Masson pine and Camphor laurel within 1500 m of the tunnel central reduced by 94.8%~135.8% and 116.6%~139.9%, respectively, while the trees beyond this distance range were less influenced. Meanwhile, the remote sensing indices showed that tunnel excavation can reduce 3.3%~7.6% of the NDVI and 15.7%~17.4% of the NPP within 1500 m of the ZMRL6 tunnel. A similar distance range of such declines in NDVI and NPP was also found in other tunneling regions throughout the karst mountain areas of Southwest China. The findings in this study suggest that tunnel excavation may cause severe ecosystem degradation within 1500 m of the tunnel center, which should be considered in ecosystem management and conservation strategies in karst mountain areas.

1. Introduction

Plants are the fundamental component of terrestrial ecosystems, providing numerous ecological, economic and social benefits across many spatial scales (Anderegg et al., 2013). Increasing vegetation cover and healthy plant function can prevent ecological risks and enhance CO_2 storage in karst areas (Cheng et al., 2015; Tong et al., 2018). The heterogeneous landform, fractured bedrock and thin soil layer make karst ecosystems extraordinarily vulnerable to environmental fluctuations (Angulo et al., 2013; Chen et al., 2018; Goldscheider, 2019). In this situation, the existence of healthy plants can reduce the related ecosystem degradation and natural hazards, because the well-developed root system of plants on karst terrain can significantly decrease soil erosion, increase microbial biomass and prevent rock desertification (Wang et al., 2004; Yan et al., 2020; Lu et al., 2022). Due to the key role of vegetation function for ecosystem stability and services in vulnerable karst areas, the knowledge for conserving and managing vegetation cover under environmental disturbances is particularly significant. In past decades, the increasing frequency of climate extremes have prominently reduced the vegetation cover and damaged plant function worldwide (Seidl et al., 2014; Gazol et al., 2020; Suratman, 2022; Liu et al., 2023). For instance, the natural extremes have resulted in tremendous negative consequences for vegetation cover and carbon stocks in the first decade of the twenty-first century (Seidl et al., 2014). Likewise, numerous studies also found that the increasing human activities and urban development have also greatly impacted the vegetation cover (Cetin and Sevik, 2016; Degerli and Cetin, 2022a; Degerli and Çetin, 2022b; Sahin et al., 2022; Aksoy et al., 2023). To date, the

* Corresponding author.
E-mail address: jiangjyj@swu.edu.cn (Y. Jiang).

https://doi.org/10.1016/j.ecolind.2023.110555
Received 27 April 2023; Received in revised form 14 June 2023; Accepted 22 June 2023
Available online 24 June 2023

negative influences of climatic extremes on the vegetation cover in karst areas has been discussed by many studies (Peng and Wang, 2012; Jiang et al., 2014), yet the knowledge of how human engineering-induced hazards affect vegetation ecosystems in karst area is still very limited. In mountainous karst areas, tunnel construction is a major human engineering project that frequently occurred in past decades (Lv et al., 2020). Numerous tunnels have been built through karst regions in response to the basic infrastructure demands of rapid local socioeconomic development in past decades. The drilling operations of these tunnels break through carbonate bedrock and aquifers below local groundwater levels (Vincenzi et al., 2009; Pesendorfer and Loew, 2010). The drawdown of the groundwater level results in the leakage of surface discharge and induces the delivery of surface water and shallow water to far below the ground, thus lowering the aquifer, shallow water and surface soil water storage (Liu et al., 2019; Cao et al., 2020). For instance, studies suggest that the excavation of tunnels may result in the losses of karst springs and wells due to the collapse of preexisting structures beneath the ground (Gisbert et al., 2009, Chiocchini and Castaldi, 2011). The alteration of hydrological conditions in vulnerable karst terrain due to tunnel excavation may threaten plant function and ecological service within the surrounding area.

The strong sensitivity of plant growth and function to changes in available water in ecosystems has been discussed in many studies (Seddon et al., 2016; Wilmking et al., 2020). Because of the rapid weathering of carbonate rock, low speed of pedogenic processes and intense human agricultural activity, the soil layer in karst areas is characterized by thin layers and poor water storage capacity (Wang et al., 1999; Wang et al., 2004; Zhang et al., 2011; Jiang et al., 2014; Lu et al., 2022). Although some karst ecosystems are located in humid climate regions, studies suggest that water for plant growth is still limited due to the limited ability of rocky soils and near-surface fractured layers to store it (Nie et al., 2011; Liu et al., 2019; Ding et al., 2021; Liu et al., 2021a). To survive in such stressful water environments, plant roots penetrate through a network of cracks or fissures that exist in fractured carbonate bedrock to extract water from the soil layers and subcutaneous zone and even from deep underground rivers (Mccole and Stern, 2007; Querejeta et al., 2007; Nie et al., 2011; Estrada-Medina et al., 2013; Heilman et al., 2009; Heilman et al., 2014). The dimorphic root system is significant for tree species growing on karst because the soils are deficient in water to support plant growth (Hasselquist et al., 2010). However, this water strategy for trees in karst areas may be greatly affected by the surface water losses and groundwater level drawdown caused by tunnel excavation. Thus, similar to the climatic drought-induced water stress events in arid or semiarid regions, the reduced water availability caused by tunneling in karst areas is likely to cause reductions in the plant growth rate (Zheng et al., 2017; Behzad et al., 2022).

The long lifespan and wide global distribution of forests allows tree rings to enhance our understanding of past and contemporary forest growth, carbon stock and water dynamics (Babst et al., 2014; Frank et al., 2015; Che et al., 2023) since tree-ring samples indicate how much wood is formed via its stems, which can be directly related to biomass gain and carbon storage. The variations in tree-ring records can indicate the rate of growth, state of health and mortality of trees under water stress events (Cailleret et al., 2017; Park Williams et al., 2013). Hence, dendrochronology has been used in recent studies to monitor plant growth under tunneling-induced surface water depletion in karst areas (Zheng et al., 2017; Behzad et al., 2022). Indeed, the radial growth of trees offers long-term information on forest growth before and after tunnel construction, quantifying the decline and recovery of tree growth and health in different periods. However, previous studies still have not fully determined the range of distance to which a tunnel may cause ecological damages, such as negatively impact forest growth. Therefore, it would be useful to examine the response of radial growth at different distances from a tunnel center. In addition, although tree rings provide an accurate and retrospective measure of tree growth, their use involves intensive field work to collect wood samples and requires numerous tree species to present the general response of forest ecosystems to environmental perturbations (Vicente-Serrano et al., 2016). Meanwhile, due to the limitation of tree cores, tree-ring series only reflect forest responses to water stress events at local scales (Xu et al., 2019), while the responses of other vegetation types are not documented. Therefore, the use of only the spatial coverage of tree-ring data may limit the accuracy of estimating tunneling-induced ecological damage in mixed vegetation cover ecosystems. Remote sensing indices, such as the Normalized Difference Vegetation Index (NDVI), contribute to the realization of continuous spatial–temporal observations of vegetation canopy greenness (Asner et al., 2016) and have been used to estimate the Net Primary Production (NPP) for terrestrial ecosystems. Recent studies suggest that tree-ring width is strongly related to NDVI and NPP and that these two indices can also be considered indicators of plant growth, providing references for plant function and health (Piao et al., 2006; Raynolds et al., 2008; Berner et al., 2011; Vicente-Serrano et al., 2016; Xu et al., 2019; Suratman, 2022; Liu et al., 2023). Compared to traditional field measurements (tree-ring records), often taken for specific trees, the vegetation productivity driven by remote sensing (NDVI and NPP) can provide an overall assessment of growth across all vegetation types at a much greater spatial extent with continuity, offering an advantageous technique to evaluate ecological damage caused by water stress events (Breshears et al., 2005; Zhao and Running, 2010; Brun et al., 2020; Suratman, 2022; Liu et al., 2023). For instance, the tree ring width and and NDVI has been synthetically used to detect the response of forest growth to drought in Spain (Gazol et al., 2020). Moreover, the NDVI and NPP has been applied to detect the dynamics of plant growth under drought and climate factors in Central Asia (Liu et al., 2023). Although studies suggested that the remote sensing indices can be an additional tool for estimating the influences of human activities on plant growth, it is still lack of case studies which can develop this method to describe and quantify the ecological damages induced by tunnel excavation.

Currently, a growing number of studies have proved that the combined use of remote sensing indices and the GIS buffer zone can be an effective method to evaluate the impacts of different human activities on vegetation cover (Cetin, 2015; Cetin et al., 2021; Aksoy et al., 2023). For example, Aksoy et al. (2023) found that wind turbines in the Urla, Çeşme, and Karaburun peninsulas have significantly damaged the surrounding vegetation cover. Such negative influences were strongly related to the distances that were close to the turbines. Considering that the wind turbines and tunnels can both be classified as human engineering structures, therefore, we believe the combined application of remote sensing indices and the GIS buffer zone analyze may become an innovative and appropriate methodology for evaluating the response of plant growth to tunnel excavation in karst areas. Besides, the vulnerability and recovery of plant growth under drought events are different between species and compositions. (Bowman et al., 2013; Aldea et al., 2022; Che et al., 2023). Thus, the recovery of plant growth after tunnel excavation may also vary among species and vegetation types. In this case, tree-ring data still has the advantage of evaluating the responses of growth between different species within a single vegetation cover type, because this method provides more accurate data and covers a longer time span than remote sensing methods. In addition, to further detect the characteristics of tunneling-induced ecological damages, using the GIS buffer zone to analyze tree-ring data is also an innovative endeavor. Therefore, we assume that the combined use of tree-ring records, remote sensing indices, and the GIS buffer zone analysis may offer an efficient and cost-effective approach for drawing a comprehensive view of tunneling-induced ecological damage, which could help in developing ecosystem management and conservation strategies in the future. In this study, we aim to address the following questions using tree-ring records and remote sensing vegetation indices: (1) what is the distance range for which tunneling may affect radial growth in karst area? (2) How does tunnel excavation change the NDVI and NPP within the surrounding karst area? To achieve these goals, we used an unstandardized basal area

increment (BAI) series of tree-ring widths from two dominant tree species (Masson pine and Camphor laurel) around a typical tunnel located in a karst trough valley in Southwest China to evaluate the response of forest growth under tunnel excavation. In addition, the variations in NDVI and NPP were analyzed by the GIS buffer zone tool to estimate the response of overall plant growth for tunnel excavation at this site. Furthermore, we detected the dynamics of these remote sensing indices in 91 tunnels (constructed in 2013) in the karst trough valley of Southwest China. We believe these studies may offer insights for ecosystem management and conservation in karst tunneling regions in the future.

2. Materials and methods

2.1. Study site

The Zhongliang Mountain Karst Trough Valley is located in northwestern Chongqing, Southwest China (106°23′15″~106°28′05″E, 29°40′30″~29°48′10″N, Fig. 1), and has a surface area of 37.2 km^2. The study area is dominated by a subtropical humid monsoon climate with an annual average temperature of 21.3℃. The annual average precipitation of the area is 1200 mm, 75 ~ 85% of which occurs in the plant growing season (May to October). The trough valley is mostly covered by forest and cropland. The major tree species of the study site are mixed evergreen broad-leaved trees, including Masson pine (*Pinus massoniana*), Camphor laurel (*Cinnamomum camphora*), Chinese fir (*Cunninghamia lanceolata*), and Schima superba (*Chinese Gardn. and Champ.*). Most trees were seeded between the 1980s and 1990s.

The Zhonglian Mountian Karst Trough Valley was formed by well-developed karst limestone with a thickness of 500–700 m and is surrounded on two sides by nonkarst (sandstone and mudstone) ridges with a thickness of 170–1100 m. The terrain of the basin consists of three mountains with two karst trough valleys, and the elevations of the mountains range from 200 to 700 m. All the mountains are located in the Guanyinxia anticline. The core of the anticline is a karst aquifer composed of limestone, and the strata are the Lower Triassic Feixianguan Formation (T_1f). The formations on both sides of the anticline core are the middle series of the Leikoupo Formation (T_2l) and the lower series of the Jialing River Formation (T_1j). The formations on the two sides of the valley are the Upper Triassic Xujiahe Formation (T3*xj*) and Lower Jurassic Pearl Chong Formation (J_1z), where the lithologies are feldspar-quartz sandstone, shale and mudstone (Li et al., 2021). The valley has various karst landscapes, including open crevices, sinkholes, shafts at the surface, channel conduits, small caverns, and underground rivers (or cave streams) at depth. These features provide a fast transfer of rainwater and surface water into karst aquifers below and ultimately to underground rivers, limiting water storage of plant-available water-source pools in shallow zones (Rong et al., 2011; Estrada-Medina et al., 2013; Yang et al., 2016).

There are three tunnels located in the Zhongliang Mountain karst trough valley. In this study, we focused on one tunnel that was built in the 2010s. The project of the Zhongliang Mountain Railway Line 6 (ZMRL6) tunnel in Beibei District of Chongqing City was started in 2010 (drilling of the tunnel) and finished in 2013 (completely constructed). The reason for selecting this tunnel is its construction period and location. The other two tunnels have average linear distances of ~ 1500 m and ~ 3000 m with the ZMRL6 tunnel (on the northern part of the valley). The ZMRL6 project has a nearly 9-year time gap with the closest tunnel (Beibei tunnel of Yuwu Expressway). There are no adjacent tunnels (<9000 m) in the southern part of the ZMRL6 tunnels. In addition, the surrounding area of the ZMRL6 tunnel has available high-resolution remote sensing datasets and modern records. Previous field investigations found that the construction of the ZMRL6 tunnel has drastically reduced the surface water resources in Zhonglian Mountain Karst Trough Valley. Before tunnel excavation, numerous springs and wells were available for domestic water supply and agricultural irrigation in the surrounding village. However, spring and well discharges suddenly declined or dried up after the tunnel within the study site was excavated. The discharge of springs used to be a major water source for the local community before tunnel construction. To date, the humans

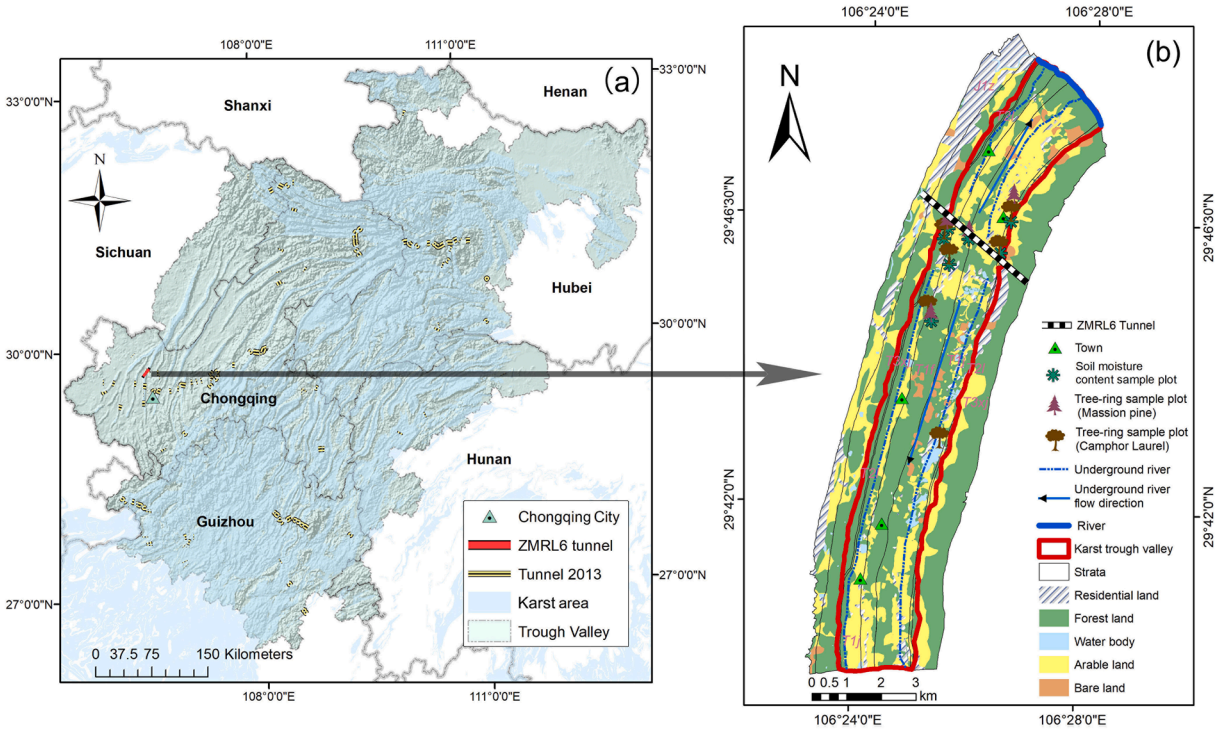

Fig. 1. Location of the study site. The map (a) shows the location of the Zhongliang Mountain Railway Line 6 (ZMRL6) tunnel and the distribution of 91 tunnels in the karst mountain areas of Southwest China (constructed in 2013). The map (b) shows the spatial information of the tunnel, land use, hydrological information, soil moisture content sample sites and tree-ring sample sites in the Zhongliang Mountain Karst Trough Valley.

and livestock around the ZMRL6 tunnel, however, became fully dependent for drinking water on the surface water pumped from the excavated tunnels and Jialing River or on the water from local waterworks (Liu et al., 2019). Similarly, the declines of soil moisture content is another key evidence for indicating the surface water depletion due to tunnel excavation. In Zhonglian Mountain Karst Trough Valley, there were remarkable differences in soil moisture contents between the tunnel-affected areas and the areas that unaffected by tunnel excavation, indicating that groundwater drawdown resulted from tunneling decreased the soil water availability around the ZMRL6 (Cao et al., 2020; Behzad et al., 2022). In addition, previous survey found that the vegetation coverage within the ZMRL6 tunnel has become relatively poor, and regional rocky desertification worsened after the tunnel construction (Liu et al., 2019). Therefore, the time of construction, locations, surface water depletion and rock desertification make the ZMRL6 tunnel a perfect site for studying the distance range of ecological damages caused by tunnel excavation.

2.2. Methods

2.2.1. Soil sampling and soil moisture content analysis

To detect the distance range for which tunneling may affect plant growth in karst areas is one of the main targets of this research. The spatial variations of soil water storage around the tunnel can provide key evidences, demonstrating the areas that tunneling may induce water stress and stunt plant growth. Therefore, before studying the spatial changes in growth rate around the ZMRL6 tunnel, we conducted further investigations of the soil moisture contents (SMC) in Zhongliang Mountain Karst Trough Valley. We collected the soil samples at the depths of 0–20 cm and 20–40 cm in different distances (500 m, 1000 m, 1500 m and 2500 m) around the ZMRL6 tunnel center during January 2021 to analysis the spatial variation of soil moisture contents (Table 1 and Fig. 1). The soils were taken in two depths of each location and both sampling sites were close to the target plants (tree ring) which we intended to analysis. The gravimetric soil moisture contents (SMC, %) of each soil samples were determined by drying at 105℃ in the oven for 24 h.

2.2.2. Tree-ring width sampling and processing

The widths from a series of annual growth rings can capture long-term interactions between tree growth and water sources (Ferguson and George, 2003; Zweifel et al., 2006; Creutzfeldt et al., 2015; Berdanier and Clark, 2018). Therefore, many studies applied tree-ring to detect how the growth rates of plants respond to natural or anthropogenic water stress events (Cailleret et al., 2017; Park Williams et al., 2013; Behzad et al., 2022). In this study, to capture a more general view of the impacts of tunneling-induced water stress events on the growth rates of trees within the ZMRL6 tunnel at different linear distances, we selected two of the most common tree species around the ZMRL6 tunnel, Masson pine and Camphor laurel, and obtained their tree-ring cores from the tree stands in different buffer zones (the buffer zone is a GIS concept; it is a region drawn around the lines/polygons that encompasses all of the areas within a specified distance) around the tunnel center. The reason for selecting these two different species of tree stands is to show the difference in stress-driven responses for different types of species of tree stands (Bowman et al., 2013). Because different tree species may perform distinct tolerances that dictate how they respond to natural and anthropogenic disturbances, such as water stress events (Eilmann and Rigling, 2012; Gazol et al., 2020; Behzad et al., 2022). For instance, it is suggested that coniferous trees are more drought-tolerant to natural extremes than broad-leaved trees (Cao et al., 2021). In Zhongliang Mountain Karst Trough Valley, The dominant local coniferous tree is Masson pine, while the dominant local broad-leaved tree is Camphor laurel. Meanwhile, these two tree species also have the most appropriate tree stands for tree-ring sampling. Therefore, we believe the comparative analysis of these two representative species is necessary. Because this not only can draw a more general view of the tunneling-induced ecological damages but also could help to make specific plant species conservation strategies in the future.

Thus, we obtained tree-ring cores from mature forests within 0–500 m, 500–1000 m, 1000–1500 m, 2000–2500 m and > 6000 m around the ZMRL6 tunnel. The details of the tree sample locations are shown in Fig. 1 and Table 1. These tree cores were taken at ~ 1.3 m in height using a 5.144 mm increment borer from different directions and were stored in a customized quartz glass tube. Then, all the tree cores were air-dried and mounted onto grooved boards. Afterwards, the samples were sanded with P1000 (ISO/FEPA grit designation) sandpaper until the annual ring boundaries were clearly visible for each core. The prepared cores were cross-dated to find possible missing or false rings and to obtain a true calendar year via LINTAB and software TSAP Win (Stokes and Smiley, 1996; Behzad et al., 2022). Due to the weaker dependence on tree age, the Basal area increment (BAI) series was used in this study instead of the ring-width series to obtain more accurate and reliable information regarding the growth dynamics of the tree stands and their water source (Schuster and Oberhuber, 2013; Obojes et al., 2018). The BAI series of tree rings can be calculated by the following (Jump et al., 2006):

$$BAI = \pi(R_t^2 - R_{t-1}^2) \quad (1)$$

where R and t correspond to the tree radius and date of tree-ring formation for an individual tree, respectively. Accordingly, a plot-by-plot analysis of different buffer zones was conducted using the BAI series of Masson pine and Camphor laurel around the ZMRL6 tunnel to track negative growth signals linked to tunnel excavation when the stand BAI level shifted from a positive to a negative trend during the tunnel excavation event. This method can also demonstrate the different influences of tunnel excavation on tree growth along the distance.

2.2.3. Remote sensing data sources and NDVI

Remote sensed spectral indices are widely applied to quantify vegetation structure and functioning (Asner et al., 2016). The normalized difference vegetation index (NDVI) can reflect the changes in vegetation canopy greenness (Cohen et al., 2016). The net primary productivity (NPP) quantifies the amount of atmospheric carbon fixed by plants and accumulated as biomass (Zhao and Running, 2010). These two parameters can reflect the plant's growth across different biomes. In this study, three years of remote sensing images produced by Landsat were used to monitor the dynamics of the land use and vegetation index before and after the construction of the ZMR6 tunnel. Landsat images were downloaded from the Land Processes Distributed Active Archive center, LP DAAC/NASA. The remote sensing images were spatially corrected and radiometrically calibrated before processing. The selected multispectral remote sensing images (including the images of all months within one year) were taken before tunnel excavation (2009), during tunnel construction (2013), and after tunnel construction (2015). To identify and classify the land use in the Zhongliang Mountain Karst

Table 1
The location of soil and tree ring sampling around the Zhongliang Mountain Railway Line 6 (ZMRL6) tunnel.

Distance	Sample location	
	Soil and Camphor laurel	Soil and Masson pine
0–500 m	106.43949,29.76827#	106.430563,29.772214#
500–1000 m	106.41676,29.77318#	*
1000–1500 m	106.44268,29.77747#	106.420365,29.776541#
1500–2000 m	106.42478,29.765751@	106.443459,29.782064@
2000–2500 m	*	106.420133,29.750457#
>6000 m	106.42404,29.71798@	*

Note (1): # indicates the locations for both soil and tree-ring sampling and @ are the sites for tree ring sampling only.
Note (2): *Indicates missing samples in the area.

Trough Valley, the selected remote sensing images were displayed in a false colour combination mode of 432 bands. Under this display mode, the natural vegetation (forest, shrub, grass and crop) in the remote sensing images is bright red and dark red, the water body is blue–black, and the bare land (bare rock, bare soil and residential land) is light red. According to these different spectral signatures, land use was simply divided into three categories. The NDVI before and after tunneling for the study area was calculated with the following formula:

$$NDVI = (NIR - R)/(NIR + R) \quad (2)$$

where NIR and R indicate reflectance in the near-infrared (NIR) and red bands, respectively. The monthly Landsat images were processed in ENVI software with a resolution of 30 m by using the maximum value composites method to calculate NDVI. The NPP of this study was calculated by the CASA model. To estimate the impacts of tunnel excavation on the vegetation dynamics in all other tunneling regions (tunnels also built in 2013) in the whole karst trough valley of Southwest China, we also downloaded the long-term MODIS NDVI (MOD13A3) and NPP (MOD17A3) data (2000–2019) from LP DAAC/NASA. The resolutions of NDVI and NPP for large-scale estimation are 250 m and 500 m, respectively.

2.2.4. The estimation of NPP

The Carnegie-Ames-Stanford Approach (CASA) model was developed based on the principle of light use efficiency (LUE) and is commonly used to simulate NPP (Potter et al., 1993; Li et al., 2018). The NDVI, temperature, precipitation, solar radiation, and soil physical property data were used to drive the CASA model. The NPP of vegetation can be simulated through environmental factors, such as NDVI, temperature, precipitation and solar radiation. The CASA model assumes that the NPP is directly proportional to the product of the absorbed photosynthetic effective radiation (*APAR*) and the maximum optical utilization efficiency (ε^*). The model calculates *APAR* as a linear function of solar radiation. This relationship exists between the fraction of absorbed photosynthetically active radiation and the reflectance property represented by the vegetation index (NDVI). The details of the CASA model are presented as follows:

$$NPP(x,t) = APAR(x,t) \times e(x,t) \quad (3)$$

where x is the spatial position of the pixel and t is the time. *APAR* is the photosynthetically active radiation absorbed by the plant (MJ m^{-2} mon^{-1}), and ε is the actual light utilization (gC MJ^{-1}).

$$APAR(x,t) = SOL(x,t) \times FPAR(x,t) \times 0.5 \quad (4)$$

$$FPAF(x,t)SR = \frac{(SRx,t - SR_{i,min}) \times (FPAR_{max} - FPAR_{min})}{(SR_{i,max} - SR_{i,min})} + FPAR_{min} \quad (5)$$

$$SR(x,t) = \frac{1 + NDVI_{(x,t)}}{1 - NDVI_{(x,t)}} \quad (6)$$

where *SOL* (*x,t*) represents the total solar radiation of pixel x in month t, *FPAR* (*x,t*) represents the proportion of *APAR* absorbed by vegetation of pixel x in month t, and 0.5 is a constant, indicating that the effective solar radiation absorbed by vegetation is half of the total solar radiation.

$$\varepsilon(x,t) = T_{\varepsilon 1}(x,t) \times T_{\varepsilon 2}(x,t) \times W_{\varepsilon}(x,t) \times \varepsilon^* \quad (7)$$

where $T_{\varepsilon 1}$ (*x, t*) and $T_{\varepsilon 2}$ (*x, t*) are temperature stress coefficients, W_{ε} (*x, t*) is the water stress coefficient, and ε^* is the maximum value of the light-use efficiency rate. The vegetation index for the CASA model employed the monthly NDVI that we calculated in the previous section, and the climatic inputs were downloaded from a local meteorological station.

2.2.5. The digital distribution of the tunnels

To detect the dynamics of remote sensing indices around the tunnels in other karst mountain areas of Southwest China, we collected digital data for the tunnels that were constructed between 2010 and 2013 within the whole karst trough valley (Supplementary Table 1). The digital map of karst distribution in Southwest China was provided by the Karst Institute of Geology, Chinese Academy of Geological Sciences (https://www.karst.cgs.gov.cn/). The spatial data of tunnels in the areas of Southwest China are freely accessed on the Open Street Map website (https://www.openstreetmap.org/). The digital data for other tunnels were created in the GIS environment according to the spatial information (location, length, etc.) we collected.

2.2.6. Data analysis methods

To quantify and describe the impacts of human activities on the vegetation cover, the conventional method is currently not enough. Previous studies constructed an effective and successful methodology by combining remote sensing technology and the GIS buffer zone analysis (Cetin, 2015; Cetin et al., 2021; Aksoy et al., 2023). This method built equidistant buffer zones (a region drawn around the lines/polygons that encompasses all of the areas within a specified distance) around man-made structures, and evaluated the changes in vegetation cover within the zones by calculating the variations of all pixels (remote sensing indices) in it. Thus, to further prove the findings of tunneling-induced ecological damages that indicated by tree-ring data, we adopted this new method. Considering that tunnels can be spatially analyzed by GIS as a vector (polyline in ArcGIS) format, we drew the ZMRL6 tunnel and all the other tunnels that we listed in Supplementary Table 1, and constructed different buffer zones with these line data by using the buffer zone analysis tool in ArcGIS 10.2. Meanwhile, we calculated the mean values of all remote sensing indices (pixels) or estimated their linear trends within the buffer zones during different tunnel impact periods (tunnel construction periods and post-tunneling periods). By comparing the changes in remote sensing indices for different buffer zones and periods, we can consequently detect the distance range for which tunneling may affect plant growth in karst areas. Also, these results can further be verified the BAI trends of Masson pine and Camphor laurel, because the tree-ring samples also came from the different buffer zones that we built. Meanwhile, the trends of BAI and remote sensing indices (NDVI and NPP) were all analyzed by linear regression methods in SPSS Statistics 20 or via GDAL (Python Package). The significance of regression was tested by the Pearson correlation coefficient.

3. Results

3.1. The spatial changes in soil moisture contents around the Zhongliang Mountain Railway Line 6 (ZMRL6) tunnel

As shown in Table 2, the results showed that the SMC among the distances around the ZMRL6 tunnel were significantly different, whereas the values from two soil depths at the same distances were similar. From 500 m to 1500 m, the SMC gradually increased from 23.99% to 34.52% at 20 cm and from 23.1% to 30.01% at 40 cm. Meanwhile, the SMC showed no clear differences between the locations of 1500 m and 2500 m. The obvious differences of SMC from different sites around the ZMRL6 tunnel indicated that tunnel construction decreased the soil water storage on land surface within a specific

Table 2
The soil moisture contents (SMC) from different soil depths around the Zhongliang Mountain Railway Line 6 (ZMRL6) tunnel.

Distance	Soil moisture content (SMC, %)	
	20 cm	40 cm
500 m	20.73%~27.25%	19.04%~27.07%
1000 m	27.01%~31.08%	31.41%~34.91%
1500 m	31.99%~37.05%	26.19%~33.96%
2500 m	30.99%~37.67%	30.07%~33.31%

distance range (~1500 m).

3.2. The spatial–temporal changes in BAI for Masson pine and Camphor laurel around the Zhongliang Mountain Railway Line 6 (ZMRL6) tunnel

As shown in Fig. 2 and Table 3, the BAI trends of Masson pine in different buffer zones around the ZMRL6 tunnel were different throughout the study period. Although the long-term Masson pine BAI for buffer zones > 1500 m demonstrated general increasing trends from the 1980s to 2010s, the BAI changes for areas < 1500 m can be divided into two rate periods. The growth rate for BAI before 2010 was positive, at approximately 0.53 a^{-1}, while the growth rate for BAI after 2010 was negative, at −0.19 a^{-1}. Similarly, the BAI of Masson pine in the 1000–1500 m buffer zone presented an increasing trend of approximately 0.97 a^{-1} prior to 2010 and a decreasing trend of 0.05 a^{-1} during 2010–2020. In contrast, the growth rate of BAI at approximately 1500–2000 m from the tunnel was 0.69 a^{-1} before 2010 and 0.59 a^{-1} during 2010–2020.

Fig. 3 and Table 4 demonstrated the variations in BAI for Camphor laurel in different buffer zones around ZMRL6. The BAI trends of Camphor laurel from different buffer zones presented overall increasing trends during the 1980s–2010s. However, the areas closer to the central tunnel presented more negative BAI trends after a year of tunnel drilling. Before 2010, the average growth rates of BAI in the ranges of 0–500 m, 500–1000 m and 1000–1500 m were 2.03 a^{-1}, 3.17 a^{-1} and 3.37 a^{-1}, respectively. Later, these rates inversely decreased below zero, ranging from −0.56 a^{-1} ~ −0.86 a^{-1}. Similar increasing BAI growth rates occurred in the buffer zones of 1500–2000 m and > 6000 m. Before 2010, the growth rate in the buffer zone of 1500–2000 m was 0.96 a^{-1}; this rate increased to 1.29 a^{-1} after tunnel excavation. The BAI of Camphor laurel in the buffer zone > 6000 m showed remarkable increasing trends before and after 2010, which were 2.46 a^{-1} and 4.09 a^{-1}, respectively.

3.3. The changes in land-use, NDVI and NPP before and after the Zhongliang Mountain Railway Line 6 (ZMRL6) tunnel excavation

The proportion of the area occupied by each type of land use was calculated by using the supervision classification results of two periods of Landsat images (2009 and 2013). The surface water body and natural vegetation in the study area markedly decreased after the excavation of the ZMRL6 tunnel. The proportion of bare land area increased from 32.94% to 39.67%, with a value of approximately + 6.73%. According to the zonal statistics (Fig. 4 and Table 5), we found that the NDVI trends in buffer zones were different along the distance. From 2009 to 2013 (tunnel excavation period), the NDVI value in the buffer zone of 0–500 m decreased from 0.6302 to 0.5822. In the area approximately 500–1500 m from the central tunnel, the NDVI value presented a similar decreasing trend. During 2013–2015 (after tunnel excavation), the NDVI within 0–1500 m of the tunnel inversely increased by approximately 0.09. In contrast, in the buffer zone of 1500–2000 m, the NDVI value showed an overall increase, and no different trends were found before and after tunnel excavation. Meanwhile, the NPP around the ZMRL6 tunnel demonstrated similar changes with NDVI (Fig. 4). As shown in Table 6, the NPP in the buffer zone 0–500 m decreased from 545.21 gC $m^{-2}a^{-1}$ to 469.89 g C/m^{-2}(−|-)a^{-1} during the tunnel construction period (2009–2013). Decreasing NPP trends have also been found in the buffer zones of 500–1000 m and 1000–1500 m. The NPP in the buffer zones < 1500 m was inversely increased during 2013–2015. In contrast, the NPP trends in the area > 1500 m showed consistent increasing trends from 2009 to 2015.

3.4. Influence of tunnel excavation on NDVI and NPP in the karst trough valley of Southwest China

Our case study in the Zhongliang Mountain Karst Trough Valley (around the ZMRL6 tunnel) indicated vast changes in NDVI and NPP after tunnel excavation. To further explore such influences for tunneling regions in the other karst mountain areas of Southwest China, we collected the spatial information of 91 tunnels that were excavated in 2010 and completely constructed in 2013. We analyzed the changes in NDVI and NPP from the MODIS satellites within the surrounding area of these tunnels. The distribution and detailed information of these tunnels are shown in Fig. 1 and Supplementary Table 1 (Supporting Information). We used the NDVI (MOD13A3) and NPP (MOD16A3) data from 2010, 2013 and 2018, which represent the construction period (2010–2013) and post-tunneling period (2013–2018), respectively. By using the buffer analysis tool of ArcGIS 10.2 software, five buffer zones

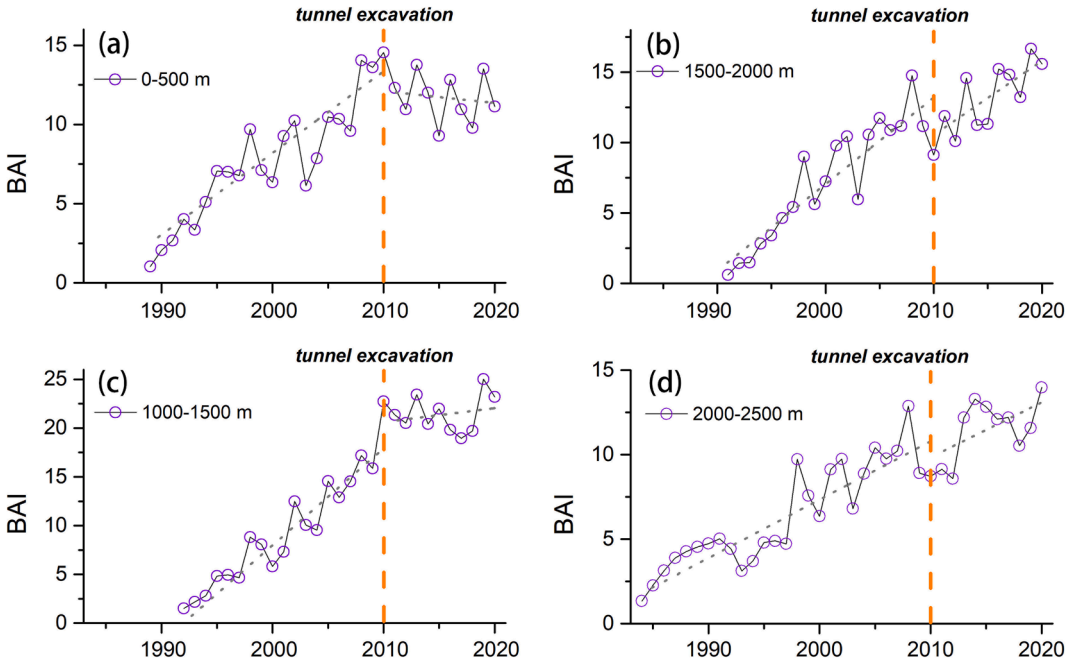

Fig. 2. BAI of Masson pine in different buffer zones of the Zhongliang Mountain Railway Line 6 tunnel (ZMRL6).

Table 3
Statistics of Masson pine BAI in different buffer zones of the Zhongliang Mountain Railway Line 6 tunnel (ZMRL6).

Buffer zone	0–500 m	500–1000 m	1000–1500 m	1500–2000 m	2000–2500 m	>2500 m
Average growth rate	0.33	*	0.84	0.47	0.30	*
Growth rate before 2010	0.53	*	0.97	0.69	0.36	*
Growth rate after 2010	−0.19	*	0.05	0.59	0.37	*

Note: *Indicates missing samples in the area.

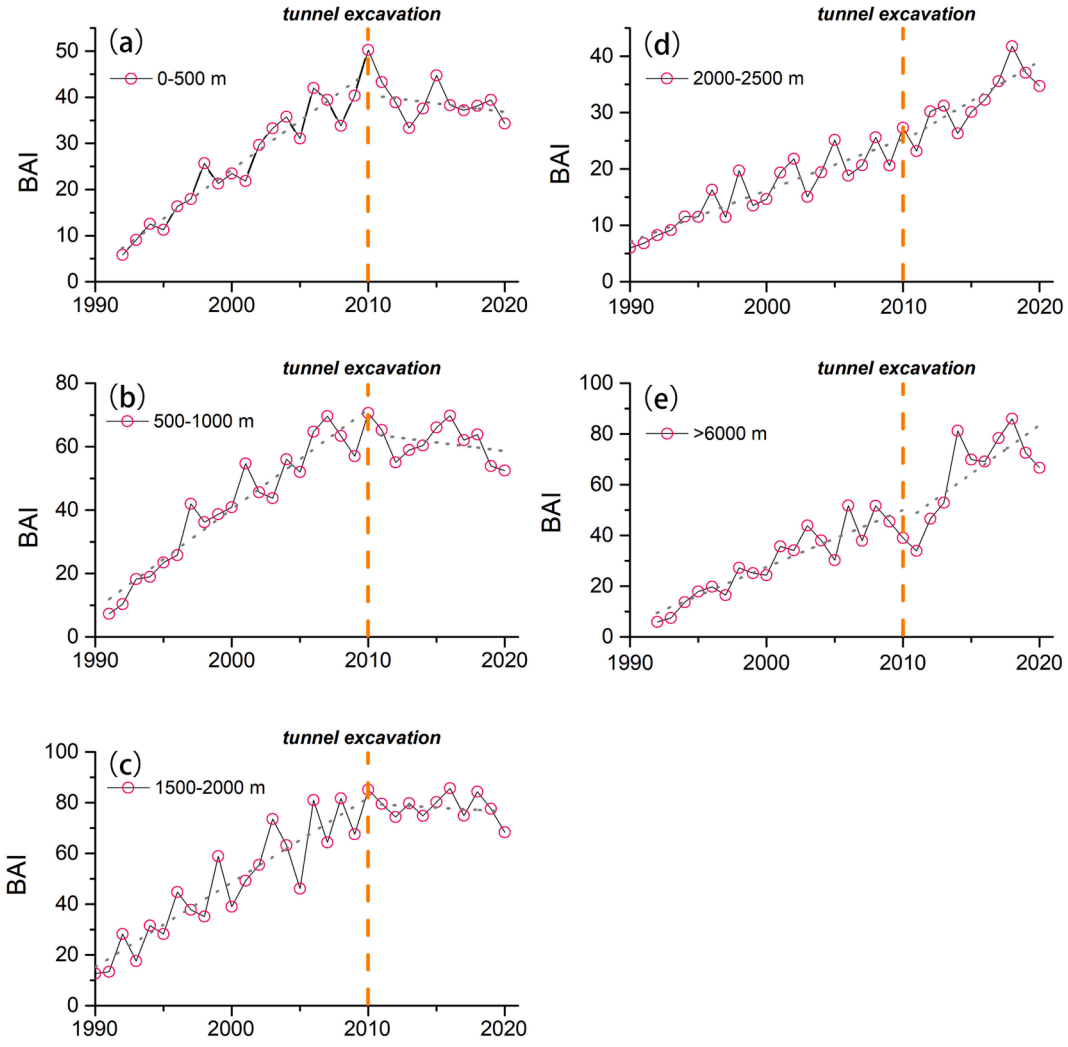

Fig. 3. BAI of Camphor laurel in different buffer zones of the Zhongliang Mountain Railway Line 6 tunnel (ZMRL6).

Table 4
Statistics of Camphor laurel in different buffer zones of the Zhongliang Mountain Railway Line 6 tunnel (ZMRL6).

Buffer zone	0–500 m	500–1000 m	1000–1500 m	1500–2000 m	>6000 m
Average growth rate	1.15	1.75	2.47	1.02	2.47
Growth rate before 2010	2.03	3.17	3.37	0.96	2.46
Growth rate after 2010	−0.81	−0.86	−0.56	1.29	4.09

with 500 m intervals were established around these tunnels (0–2500 m). We applied linear regression (GDAL) to estimate the changes of NDVI and NPP for all pixels within the buffer zones during the periods of 2010–2013 and 2013–2018, respectively. Meanwhile, the increasing area of NDVI or NPP (linear trends of NDVI > 0 or trends of NPP > 0) in the tunnel buffer during the two periods was obtained by using the Zonal Statistics tool in ArcGIS 10.2.

During the tunnel construction period (2010–2013), we found that the proportion of NDVI decline areas in the buffer zones of 0–500 m, 500–1000 m, and 1000–1500 m were all higher than 50% (51.89% ~55.46%). However, in the buffer zones > 1500 m, the areas where NDVI decreased were lower than the areas where NDVI increased. The NDVI in each tunnel buffer zone showed a larger growth area than the decline area during post-tunneling period (2013–2018). The growth areas for most buffer zones were higher than 70%, while the decline area was below 30%, indicating that the NDVI in the tunneling region

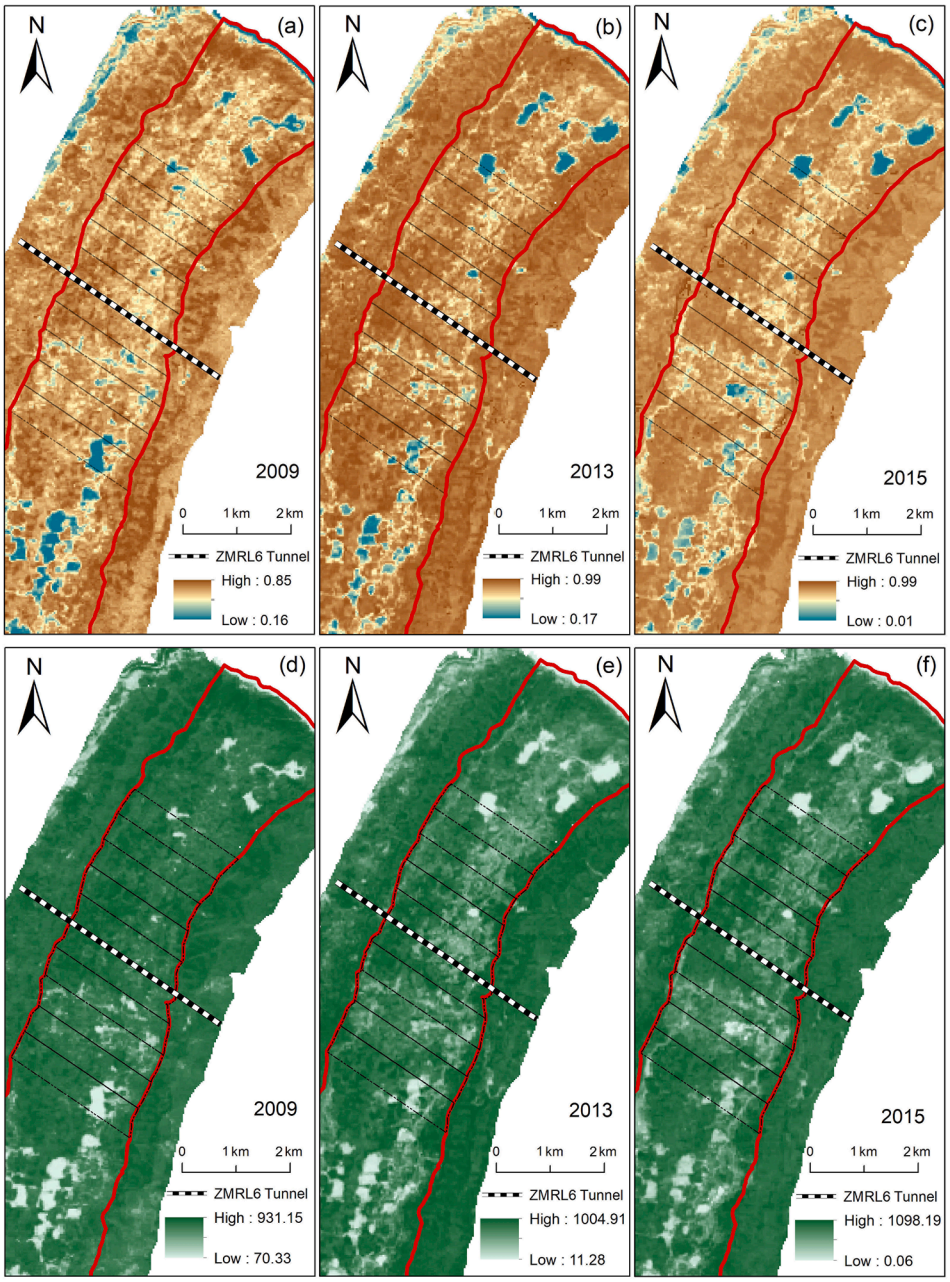

Fig. 4. NDVI and NPP of the Zhongliang Mountain karst valley during 2009–2015. Included are the NDVI in 2009 (a), 2013 (c), 2015 (d), and the NPP in 2009 (d), 2013 (e), 2015 (f). The black dashed areas are the buffer zones (interval = 500 m) around the Zhongliang Mountain Railway Line 6 tunnel.

Table 5
NDVI trends of different tunnel buffer zones around the ZMRL6 tunnel.

Year	NDVI				
	0–500 m	500–1000 m	1000–1500 m	1500–2000 m	2000–2500 m
2009	0.6302	0.6337	0.6477	0.6408	0.6224
2013	0.5822	0.6127	0.6084	0.6675	0.7162
2015	0.6007	0.6205	0.6234	0.6901	0.7418

Table 6
NPP trends of different tunnel buffer zones around the ZMRL6 tunnel.

Year	NPP (gC $m^{-2}a^{-1}$)				
	0–500 m	500–1000 m	1000–1500 m	1500–2000 m	2000–2500 m
2009	545.21	546.02	544.51	545.93	422.70
2013	458.58	450.98	459.26	464.07	508.29
2015	469.89	485.5	478.89	488.01	548.55

strongly increased after tunnel construction. Meanwhile, the NPP in the tunnel buffer zones < 1500 m also showed downwards trends during tunnel construction period (2010–2013) when compared to trends prior to tunnel construction. Within the central tunnel area of 1500 m, the proportion of NPP decline area was higher than that of growth area. The proportion of decline area was 61.36%, 57.98% and 54.77%, respectively. In contrast, during the post-tunneling period (2013–2018), the change in NPP in all tunnel buffer zones showed a significantly larger growth area than that of the decline area. In most buffer zones, the NPP increase area was >70%, while the NPP decline area was <30%. In addition, we constructed the linear regression by using the distance of different buffer zones to the tunnel center and their increasing area of

NPP and NDVI (the average values of the pixels within the buffer zone) during 2010–2013 and 2013–2018 respectively. The results showed that during the tunnel construction period of these tunnels (2010–2013), the increasing area of NDVI and NPP declined as the distance closer to the tunnel center area (Fig. 5), and Pearson correlation coefficients of the linear regressions during this period were significant (R: 0.97 ~ 0.98). By contrast, during the post-tunneling period (2013–2018), the increasing areas of NDVI and NPP for different buffer zones presented no clear differences, and no significant relationships (linear regression) and correlation coefficients can be found.

4. Discussion

4.1. The negative impact of tunnel excavation on forest growth in karst mountain areas

Generally, climate change determines the growth rate of trees, which forms the basis of dendrochronology (Esper et al., 2002; Li et al., 2006). For healthy and mature forest ecosystems, the BAI for woody plants must increase or maintain a steady level (Phipps and Whiton, 1988; Fekedulegn et al., 2003; LeBlanc et al., 1992) and is unlikely to decline before senescence (Duchesne et al., 2003; Peñuelas et al., 2008). However, studies have suggested that a decrease in BAI may occur under various water stress events, such as natural drought caused by climate extremes (Phillips et al., 2010; Lévesque et al., 2013; Barbeta et al., 2015). Hence, the BAI could be an indicator to show the response of tree growth under drought events (Muzika et al., 2004; Peñuelas et al., 2008; Obojes et al., 2018; Wang et al., 2019). However, the drastic reduction in BAI for Masson pine and Camphor laurel around the ZMRL6 tunnel (0 ~ 1500 m) after 2010 was unlikely to be caused by temperature or precipitation changes. For the Zhongliang Mountain Karst Trough Valley, there were no significant changes in the annual average temperature after the drilling operation of the ZMRL6 tunnel. The average temperature of the study site decreased by approximately 0.16 °C during 2010–2020. Pearson correlation analyses indicated that the BAIs for Masson pine and Camphor laurel showed no significant relationships with temperature around the ZMRL6 tunnel. As shown in Fig. 6, the precipitation of the study site experienced a drastic increase of approximately + 49.84 mm a^{-1}, yet the BAIs for the Masson pine and Camphor laurel demonstrated inconsistent changes within the buffer zones < 2500 m around the tunnel. No BAI data from < 2500 m of the tunnel presented a significant correlation with annual precipitation changes. There was only the sample from > 6000 m (Camphor laurel) of the tunnel showed a significant positive correlation with precipitation (R^2 = 0.66). This result implied that other environmental drivers may mainly explain the trends and spatial patterns of BAI changes in the central area around the ZMRL6 tunnel.

Numerous studies suggested that non-climatic perturbations may also decrease the radial growth rate of trees in karst areas (Bogino and Jobbágy, 2011; Zheng et al., 2017; Behzad et al., 2022). Our previous study employed long-term tree-ring records to trace the dynamics of tree growth in a typical karst trough valley and found that the changes in growth rate can partly be attributed to tunnel excavation events (Behzad et al., 2022). This was owning to the groundwater drawdown caused by tunneling and subsequent soil water content loss. As the soil is dry, plant can use groundwater and improve the water use efficiency as the soil water content decline. However, this strategy can only maintain survival, but it reduces the growth rate, because the extraction of water from depth (groundwater) in karst area is not easy and it will increase the energy cost (Ryel et al., 2010; Schwinning, 2010; Cao et al., 2020). It was no doubt that ZMRL6 tunnel is a perfect site for presenting the response of plant growth to such water stress event. Drilling of the ZMRL6 tunnel began in 2010 and ended in 2013. During this period, some paddy fields, surface water bodies, springs and wells rapidly dried up, which is evidence of surface water resource losses due to the breakage of pre-existing karst aquifers (Liu et al., 2019). In addition, the land-use data provided by the remote sensing approach presented a remarkable increase in bare land in the Zhongliang Mountain karst trough valley. These phenomena can be seemed as key indicators of groundwater level drops and shallow water losses caused by tunnel drilling operation. On the other hand, our field investigation before the tree-ring sampling showed that the SMC were rapidly declined as the soil samples approached the tunnel center (Table 2). Such condition made the ZMRL6 tunnel also an ideal site to measure the distance range that tunneling stunts plant growth. Indeed, the BAIs of Masson pine and Camphor laurel around the tunnel reflected the spatial–temporal variations of forest growth under these influences. The results not only demonstrated that the forest growth rates were stunted after tunnel excavation, but also indicated that the distance from the tunnel center may explain the spatial BAI trends and patterns. Before 2010, the BAI trends for Masson pine and Camphor laurel at approximately 0 ~ 1500 m and 0 ~ 2000 m in the ZMRL6 tunnel gradually increased, indicating that the growth of major tree species was not affected prior to tunnel excavation. When considering the fast decline of SMC from 1500 m to

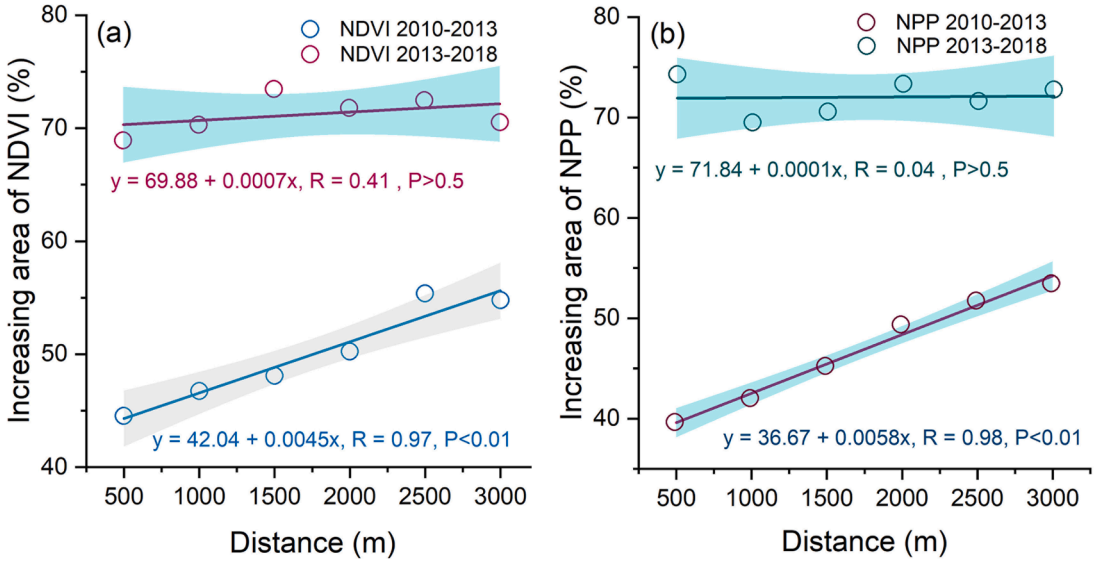

Fig. 5. the linear regressions and Pearson correlation coefficient between the distances from the tunnel center (91 tunnels constructed in 2013) and the increasing area of NDVI (a) or NPP (b) of different buffer zones in the karst mountain areas of Southwest China.

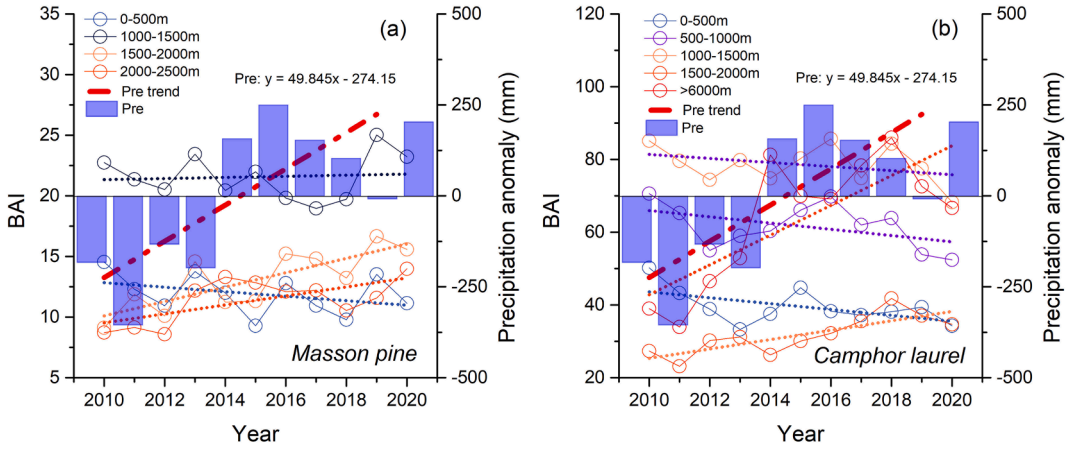

Fig. 6. Comparisons of the BAI trends of different buffer zones around the tunnel after tunnel excavation and the precipitation trend in the Zhongliang Mountain karst trough valley. (a) The BAI and precipitation trends of Masson pine. (b) BAI and precipitation trends of Camphor laurel.

the tunnel central area, the declines in BAI within such distance ranges after 2010 can undoubtedly attribute to the soil water losses induced by tunnel excavation. Moreover, throughout the study period, the consistent increase in Camphor laurel and Masson pine BAIs from buffer zones > 2000 m further confirms this distance range. The negative BAI growth rates in the buffer zones around the tunnel central area is absolutely a key piece of evidence for reflecting the distance range that tunnel may stunt plant growth. However, due to the limits of tree-ring methods, the declines of BAI of Camphor laurel and Masson pine still cannot fully reflect the overall ecological damages caused by tunnel excavation, because a large proportion of the tunneling area is covered by non-woody plants.

4.2. The dynamics of NDVI and NPP caused by tunnels excavation in karst mountain areas

Tree-ring width records provide an accurate assessment of forest growth over a much longer time series at local scales, while remote sensing data can provide a spatially continuous measure for plant growth with limited temporal coverage. Studies have suggested that climatic drought may induce an accompanying reduction in NDVI (Breshears et al., 2005; Liu et al., 2021b) as well as NPP (Zhao and Running, 2010; Liu et al., 2023). However, the NDVI and NPP (the proxies of plant growth in this study) declines we found in this study can also attribute to the surface water depletion caused by tunnel excavation instead of climatic perturbations. As we mentioned above, the construction of the ZMRL6 tunnel instead of climatic factors (temperature and precipitation) may be the key factor affecting tree growth in the Zhongliang Mountain Karst Trough Valley. According to the remote sensing approach, we found that the spatial and temporal trends of NDVI and NPP can also endorse this conclusion. Combining the changes in NDVI in some buffer zones (<1500 m) around the tunnel, it can be inferred that during tunnel construction, the drilling operation damaged the functionality of surrounding plants, which led to the decline in NDVI from 2010 to 2013 (Table 5). The NPP also demonstrated a similar declining trend in this period (Table 6). These results are consistent with the radial growth rate trends of Masson pine and Camphor laurel that we found around the tunnel (Tables 3 and 4). In addition, the tree-ring records of Masson pine and Camphor laurel indicated that the construction of the tunnel caused a decrease in tree's growth around 0 ~ 1500 m of the tunnel. According to the vegetation indices produced by remote sensing images, we found that NDVI and NPP declines induced by tunnel excavation also have a similar distance range. In addition, the decline in NDVI or NPP was higher as the buffer zones approached the tunnel center, suggesting that the negative influences of tunneling for plant growth are descending along the distance. This unique trait is similar with the changing patterns of BAI, as we presented above. The findings in Zhongliang Mountain were not specific to this particular case of tunneling-induced ecological damages because declines in NDVI and NPP have also been found in the regions of approximately 91 tunnels in the karst trough valley of Southwest China. During the tunnel construction period of these tunnels, the increasing areas of NDVI and NPP decline as the distance from the tunnel center increased (Fig. 7). After these tunnels were completely constructed (2013), the increasing areas of NDVI and NPP for different buffer zones presented no clear differences. Therefore, the variations of remote sensing indices indicated that the growth of all vegetation types (include forest) were stunted due to tunneling activities.

4.3. The distance range of tunnel induced ecological damages and the recoveries of different plants

The distance range that tunnel excavation may stunt plant growth is a major finding in this study. We believe the similar distance range (~1500 m) for SMC, BAI, NDVI and NPP declines around the ZMRL6 tunnel can be explained by the range of unrecoverable groundwater level caused by tunnel drilling operations in karst area. Previous studies found that tunnel excavation in karst area may lead nearly 10 ~ 30 m drops (with a maximum decline to > 90 m) of groundwater levels

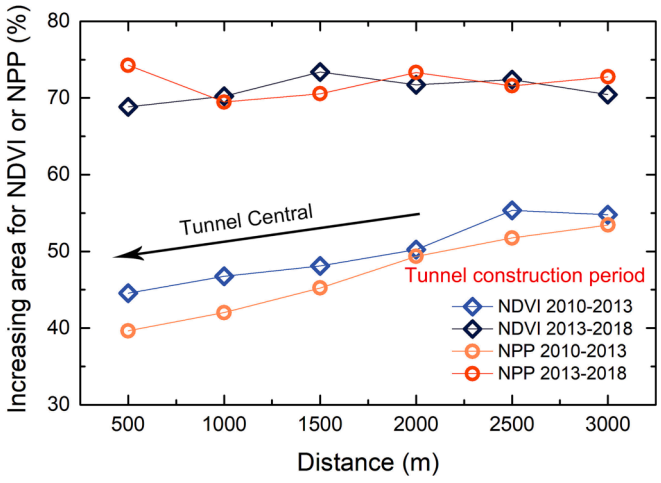

Fig. 7. NDVI and NPP changes in different buffer zones of approximately 91 tunnels in the karst mountain areas of Southwest China (completed in 2013). (a) The trends during tunnel excavation (2010–2013); (b) the trends after tunnel excavation (2013–2018).

around the center in vertical direction for years (Zheng et al., 2021; Lv et al., 2022). Meanwhile, the distance range of groundwater level drawdowns may cover approximately 2 ~ 3 km of the tunnel surrounding areas in horizontal direction, and such decreases are more obvious in the tunnel center (Lv et al., 2022). This could lead a great loss of surface water source (soil water, surface streams) in the tunneling region. For instance, Vincenzi et al. (2009) found that tunnel construction in karst areas may lead to the loss of surface streams with maximum linear distances of 1.4 km. Our results also presented a similar distance of SMC decline around the ZMRL6 tunnel. These distance ranges are close to the areas of BAI, NDVI and NPP declines we found around the tunnels in Southwest China. Therefore, we suggest that ranges of the groundwater level drawdowns may be the reasons that caused the dynamics of soil water storage and vegetation productivity (NDVI, NPP) within 1500 m of the tunnel center in karst area. According to these findings, we constructed a new conceptual diagram to better present the potential influences of tunnel excavation on local hydro-ecology in karst mountain areas, as shown in Fig. 8.

The engineering of the tunnel greatly modifies the regional groundwater system, and the subsequent changes in regolith water content may have profound impacts on the karst critical zone due to its unique hydrogeological and geochemical characteristics (Auler and Smart, 2003; Vincenzi et al., 2009; Eimil-Fraga et al., 2014). Thus, tunnel excavation may result a long-term or unrecoverable groundwater drawdown and surface water storage losses, because as the hydrological condition has been changed, restoration of groundwater field and discharge are is not possible as long as the tunnel continues to drain the aquifer (Lv et al., 2022). Hence, the magnitude of ecohydrological vulnerability to tunneling-induced water stress has been far more severe than drought-induced water stress. For some plant species, the growth rate may still decrease in mediation of extremely favorable climate conditions after tunnel excavation for years (Behzad et al., 2022). Especially for forest ecosystems, which are more sensitive and vulnerable under water stress events (McDowell et al., 2011). Thus, the growth rate of tree may not easily recover after tunnel excavation. The BAI trends of Masson pine and Camphor laurel around the ZMRL6 tunnel indicated that the steady state of tree growth has not yet been reached for the long-term following tunnel excavation, as these trends are still declining in the center area (Figs. 2 and 3). By contrast, in the area that > 6000 m of the tunnel, the BAI remarkably increased as the regional precipitation rising. This phenomenon may be attributed to the limited distance range of water level drop caused by tunnel excavation. The groundwater drawdown becomes insignificant beyond 5 km away from the tunnel center (Zheng et al., 2021). Thus, we suggest that the negative consequences of tunneling for tree growth may be profound and lasting which can own to a certain distance range of unrecoverable groundwater level drawdown. However, both trees, herbaceous understorey (or shrub) and crops contribute to NDVI and thus NPP. Therefore, the temporal trends in NDVI and NPP around the ZMRL6 tunnel may not completely agree with the dynamics of BAI (Xu et al., 2019). Unlike the trends of BAI, the NDVI and NPP slightly increased in the years after the completion of the ZMRL6 tunnel construction (Fig. 4, Tables 5 and 6), indicating that the overall ecological damage (plant growth) seemed to slowly recover. Such increases can obviously be attributed to the rising rainfall in this period because the favourable climate may increase the growth for both woody and non-woody plants. However, we still stress that the tolerance and recovery of plant growth to tunnel excavation may vary among species, and such differences need to be evaluated in future research.

4.4. *The future implications of ecosystem management and conservation in karst tunneling regions*

According to our findings in Zhongliang Mountain Karst Trough Valley and the karst tunneling regions of Southwest China, we stress that tunneling-induced water stress is as hazardous as natural drought for the health and function of vegetation cover, which needs to be treated as a great concern for local government. Meanwhile, this study may draw critical implications for ecosystem management and conservation strategies in karst tunneling regions in the future:

(1) Previous studies have proven that tree ring can been applied to evaluate the dynamics of growth rate under tunneling induced water stress event (Zheng et al., 2017; Bahzad et al., 2022). The findings in this research suggested that the comparative results of NDVI and NPP in different buffer zones also draw a similar

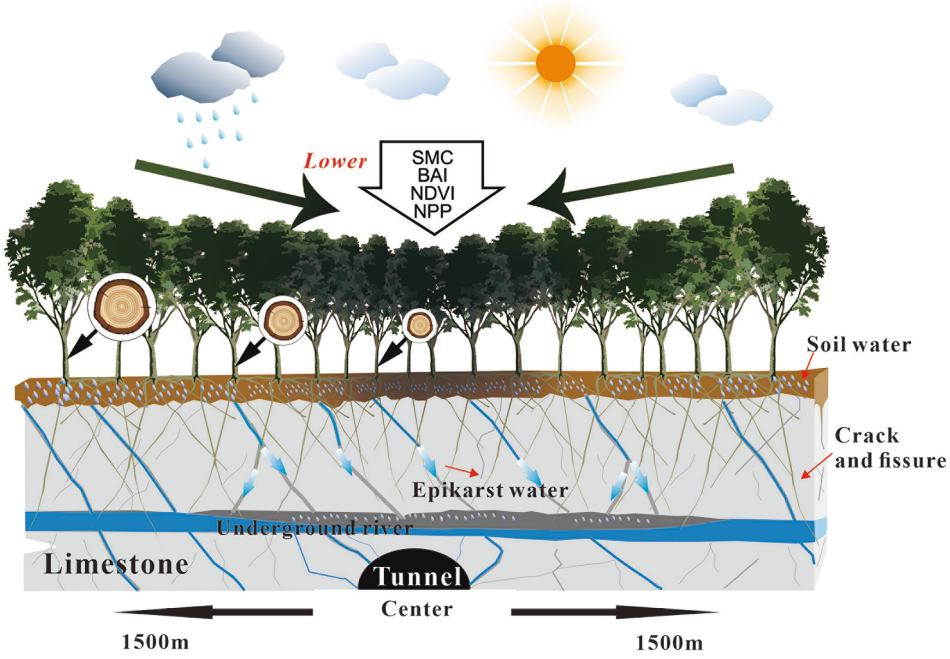

Fig. 8. Conceptual diagram of available water for plants (soil water, underground water), tree ring width, and vegetation productivity (NDVI, NPP) changes after tunnel excavation in karst mountain areas.

conclusion to the changes in tree-ring records. This not only indicated that the growth rate decline may occur in all vegetation types in karst tunneling region but also verified the combined uses of remote sensing indices and the GIS spatial analysis approach could be a convincing method for estimating the tunneling induced ecological damages. This method also offers an additional reference for the studies which intend to evaluate the ecological damage caused by other human activities. Yet, we still stress that the application of tree rings is necessary, because the forest growth rate provided by dendrochronology is more accurate and covers a more longer time span than remote sensing methods. Thus, in future research, we suggest a combination of these two complementary methodologies is crucial for providing a comprehensive reference for the tunnel induced ecological damages in karst areas.

(2) Plateaus and mountains are the dominant landforms in karst areas and act as insurmountable barriers to transportation. Tunnel excavation is necessary for efficient transportation in karst plateau and mountain areas, including motorways and railways (Lv et al., 2020). In past decades, a large number of tunnels have been built in global karst areas (countries in Asia, Europe and America). Due to the requirements of social and economic development in karst mountain areas with large populations, the demands of convenient transportation networks will inevitably rise in the future. Therefore, tunnel construction will become more frequent and widespread. Tunnel construction will not only cause a long-term reduction in water supplies for drinking, irrigation and animal husbandry but also lower plant growth, leading to the degradation of ecosystems, as presented in this study. The negative effects of tunnel excavation for plant growth and vegetation cover may extend to many socioeconomic aspects, including food production, carbon stock, human health, tourism, etc. More importantly, the high vulnerability of karst environments produces a situation in which it is very easy to damage or destroy natural resources but extremely difficult or impossible to restore conditions back to a pristine situation (Xiao and Weng, 2007). Even if remedial measures are taken, the economic costs are usually very high (Parise and Gunn, 2007). Thus, we suggest that the long-term negative impacts of tunnel excavation for vegetation cover, the tolerance of different plant species, and the economic costs for ecosystem remediation are crucial scientific questions that need to be well studied in the future.

(3) To control the ecosystem degradation and ensure the ecological service of vegetation in tunneling regions on karst terrains, we suggest that some precautionary measures can be considered in the future. Firstly, potential ecosystem management and conservation strategies in karst tunneling regions are necessary. For instance, early warning index systems and ecological risk evaluation methods should be proposed for tunnel projects with different geological structures in karst mountain areas. Moreover, new tunnels should minimize intersecting areas with strong karstification or water saturation zones. Finally, the optimal scheme of drilling operation needs to be considered before tunnel excavation to minimize the potential ecological damage.

5. Conclusion

The construction of tunnels in karst mountain areas leads to the depletion of land surface water resources, which may threaten plant function and health. Tree annual growth rings and remote sensing indices can serve as very efficient and cost-effective techniques for monitoring plant growth and health in tunneling regions. This study attempted to show how the soil moisture contents (SMC), unstandardized basal area increment (BAI), vegetation canopy greenness (NDVI) and net primary productivity (NPP) respond to tunnel excavation in different buffer zones around a central tunnel on karst terrain, thereby quantifying the ecological damage caused by this human-induced water stress event. The spatial changes of SMC in Zhongliang Mountain Karst Trough Valley indicated that tunnel excavation resulted a higher loss of soil water storage in the tunnel central area (~1500 m). The BAI series from two dominant tree species (Masson pine and Camphor laurel) around the Zhongliang Mountain Railway Line 6 (ZMRL6) tunnel suggested that the growth of trees was obviously stunted by the tunneling induced water stress event. After tunnel excavation (ZMRL6), the BAIs for Masson pine and Camphor laurel within the tunnel central 0 ~ 1500 m remarkably reduced by 94.8%~135.8% and 116.6%~139.9%, respectively, while the trees beyond 1500 m were unaffected. Moreover, the remote sensing data showed that tunnel excavation decreased the NDVI (−3.3%~−7.6%) and NPP (−15.7%~−17.4%) within 0 ~ 1500 m around the ZMRL6 tunnel. Such a distance range of NDVI and NPP declines has also been found in the surrounding regions of 91 tunnels (built in 2013) in the karst mountain areas of Southwest China. The largest declines in BAI, NDVI and NPP occurred in the central tunnel area, while these trends diminished with distance. Accordingly, we suggest that tunneling-induced water stress events may potentially stunt plant growth and damage the vegetation function and health within 1500 m around the tunnel center in karst mountain areas. The findings of this study indicates that the combined uses of remote sensing indices and the GIS spatial analysis approach could be a convincing method for estimating tunneling-induced ecological damages in karst areas. Due to the severe ecosystem degradation caused by tunnel excavation, we stress that the long-term negative impacts of tunnel excavation for vegetation cover, the tolerance of different plant species, and the economic costs for ecosystem remediation are crucial scientific questions that need to be well-studied in the future. Furthermore, potential ecosystem management and conservation strategies in karst tunneling regions are necessary.

CRediT authorship contribution statement

Sibo Zeng: Conceptualization, Methodology, Visualization, Data curation, Software, Formal analysis, Writing – original draft, Writing – review & editing. **Yongjun Jiang:** Supervision, Project administration, Funding acquisition, Conceptualization, Methodology, Writing – review & editing. **Ze Wu:** Resources, Validation, Investigation. **Caiyun Zhang:** Resources, Validation, Investigation. **Tongru Lv:** Resources, Validation, Investigation.

Declaration of Competing Interest

The authors declare that they have no known competing financial interests or personal relationships that could have appeared to influence the work reported in this paper.

Data availability

Data will be made available on request.

Acknowledgments

This work was supported by the Innovation Research 2035 Pilot Plan of Southwest University (SWU-XDZD22003)), Fundamental Research Funds for the Central Universities (SWU-KR22021) and the Chongqing Municipal Science and Technology Commission Fellowship Fund (cstc2020yszx-jcyjX0006, cstc2021yszx-jcyjX0005, 2022yszx-jcx0008cstb).

Appendix A. Supplementary data

Supplementary data to this article can be found online at https://doi.org/10.1016/j.ecolind.2023.110555.

References

Aksoy, T., Cetin, M., Cabuk, S.N., Senyel Kurkcuoglu, M.A., Bilge Ozturk, G., Cabuk, A., 2023. Impacts of wind turbines on vegetation and soil cover: a case study of Urla, Cesme, and Karaburun Peninsulas, Turkey. Clean Techn. Environ. Policy 25, 51–68. https://doi.org/10.1007/s10098-022-02387-x.

Aldea, J., Ruiz-Peinado, R., Del Río, M., Pretzsch, H., Heym, M., Brazaitis, G., Jansons, A., Metslaid, M., Barbeito, I., Bielak, K., Hylen, G., Holm, S., Nothdurft, A., Sitko, R., Löf, M., 2022. Timing and duration of drought modulate tree growth response in pure and mixed stands of Scots pine and Norway spruce. J. Ecol. 110, 2673–2683. https://doi.org/10.1111/1365-2745.13 978.

Anderegg, W.R.L., Kane, J.M., Anderegg, L.D.L., 2013. Consequences of widespread tree mortality triggered by drought and temperature stress. Nat. Clim. Change 3, 30–36. https://doi.org/10.1038/nclimate1635.

Angulo, B., Morales, T., Uriarte, J.A., Antigüedad, I., 2013. Implementing a comprehensive approach for evaluating significance and disturbance in protected karst areas to guide management strategies. J. Environ. Manage. 130, 386–396. https://doi.org/10.1016/j.jenvman.2013.08.057.

Asner, G.P., Brodrick, P.G., Anderson, C.B., Vaughn, N., Knapp, D.E., Martin, R.E., 2016. Progressive forest canopy water loss during the 2012–2015 California drought. PNAS 113. https://doi.org/10.1073/pnas.1523 397113.

Auler, A.S., Smart, P.L., 2003. The influence of bedrock-derived acidity in the development of surface and underground karst: evidence from the Precambrian carbonates of semi-arid northeastern Brazil. Earth Surf. Process. Landforms 28, 157–168. https://doi.org/10.1002/esp.443.

Babst, F., Alexander, M.R., Szejner, P., Bouriaud, O., Klesse, S., Roden, J., Ciais, P., Poulter, B., Frank, D., Moore, D.J.P., Trouet, V., 2014. A tree-ring perspective on the terrestrial carbon cycle. Oecologia 176, 307–322. https://doi.org/10.1007/s00442-014-3031-6.

Barbeta, A., Mejía-Chang, M., Ogaya, R., Voltas, J., Dawson, T.E., Peñuelas, J., 2015. The combined effects of a long-term experimental drought and an extreme drought on the use of plant-water sources in a Mediterranean forest. Glob. Chang. Biol. 21, 1213–1225. https://doi.org/10.1111/gcb.12785.

Behzad, H.M., Jiang, Y., Arif, M., Wu, C., He, Q., Zhao, H., Lv, T., 2022. Tunneling-induced groundwater depletion limits long-term growth dynamics of forest trees, 152375 Sci. Total Environ. 811. https://doi.org/10.1016/j.scitotenv.2021.152375.

Berdanier, A.B., Clark, J.S., 2018. Tree water balance drives temperate forest responses to drought. Ecology 99, 2506–2514. https://doi.org/10.1002/ecy.2499.

Berner, L.T., Beck, P.S.A., Bunn, A.G., Lloyd, A.H., Goetz, S.J., 2011. High-latitude tree growth and satellite vegetation indices: Correlations and trends in Russia and Canada (1982–2008). J. Geophys. Res. 116, G01015. https://doi.org/10.1029/2010JG001475.

Bogino, S.M., Jobbágy, E.G., 2011. Climate and groundwater effects on the establishment, growth and death of Prosopis caldenia trees in the Pampas (Argentina). For. Ecol. Manage. 262, 1766–1774. https://doi.org/10.1016/j.foreco.2011.07.032.

Bowman, D.M.J.S., Brienen, R.J.W., Gloor, E., Phillips, O.L., Prior, L.D., 2013. Detecting trends in tree growth: not so simple. Trends Plant Sci. 18, 11–17. https://doi.org/10.1016/j.tplants.2012.08.005.

Breshears, D.D., Cobb, N.S., Rich, P.M., Price, K.P., Allen, C.D., Balice, R.G., Romme, W. H., Kastens, J.H., Floyd, M.L., Belnap, J., Anderson, J.J., Myers, O.B., Meyer, C.W., 2005. Regional vegetation die-off in response to global-change-type drought. PNAS 102, 15144–15148. https://doi.org/10.1073/pnas.0505734102.

Brun, P., Psomas, A., Ginzler, C., Thuiller, W., Zappa, M., Zimmermann, N.E., 2020. Large-scale early-wilting response of Central European forests to the 2018 extreme drought. Glob. Chang. Biol. 26, 7021–7035. https://doi.org/10.1111/gcb.15360.

Cailleret, M., Jansen, S., Robert, E.M.R., Desoto, L., Aakala, T., Antos, J.A., Beikircher, B., Bigler, C., Bugmann, H., Caccianiga, M., Čada, V., Camarero, J.J., Cherubini, P., Cochard, H., Coyea, M.R., Čufar, K., Das, A.J., Davi, H., Delzon, S., Dorman, M., Gea-Izquierdo, G., Gillner, S., Haavik, L.J., Hartmann, H., Hereş, A., Hultine, K.R., Janda, P., Kane, J.M., Kharuk, V.I., Kitzberger, T., Klein, T., Kramer, K., Lens, F., Levanic, T., Linares Calderon, J.C., Lloret, F., Lobo-Do-Vale, R., Lombardi, F., López Rodríguez, R., Mäkinen, H., Mayr, S., Mészáros, I., Metsaranta, J.M., Minunno, F., Oberhuber, W., Papadopoulos, A., Peltoniemi, M., Petritan, A.M., Rohner, B., Sangüesa-Barreda, G., Sarris, D., Smith, J.M., Stan, A.B., Sterck, F., Stojanović, D.B., Suarez, M.L., Svoboda, M., Tognetti, R., Torres-Ruiz, J.M., Trotsiuk, V., Villalba, R., Vodde, F., Westwood, A.R., Wyckoff, P.H., Zafirov, N., Martínez-Vilalta, J., 2017. A synthesis of radial growth patterns preceding tree mortality. Glob. Chang. Biol. 23, 1675–1690. https://doi.org/10.1111/gcb.13535.

Cao, J., Liu, H., Zhao, B., Li, Z., Liang, B., Shi, L., Wu, L., Cressey, E.L., Quine, T.A., 2021. High forest stand density exacerbates growth decline of conifers driven by warming but not broad-leaved trees in temperate mixed forest in northeast Asia, 148875 Sci. Total Environ. 795. https://doi.org/10.1016/j.scitotenv.2021.148875.

Cao, M., Wu, C., Liu, J., Jiang, Y., 2020. Increasing leaf δ13C values of woody plants in response to water stress induced by tunnel excavation in a karst trough valley: implication for improving water-use efficiency, 124895 J. Hydrol. 586. https://doi.org/10.1016/j.jhydrol.2020.124895.

Cetin, M., 2015. Using GIS analysis to assess urban green space in terms of accessibility: case study in Kutahya. Int. J. Sust. Dev. World 1–5. https://doi.org/10.1080/13504509.2015.1061066.

Cetin, M., Sevik, H., 2016. Evaluating the recreation potential of Ilgaz Mountain National Park in Turkey. Environ. Monit. Assess. 188, 52. https://doi.org/10.1007/s10661-015-5064-7.

Cetin, M., Aksoy, T., Cabuk, S.N., Senyel Kurkcuoglu, M.A., Cabuk, A., 2021. Employing remote sensing technique to monitor the influence of newly established universities in creating an urban development process on the respective cities, 105705 Land Use Policy 109. https://doi.org/10.1016/j.landusepol.2021.105705.

Che, C., Xiao, S., Peng, X., Ding, A., Su, J., 2023. Radial growth of Korshinsk peashrub and its response to drought in different sub-arid climate regions of northwest China, 116708 J. Environ. Manag. 326. https://doi.org/10.1016/j.jenvman.2022.116708.

Chen, Z., Hartmann, A., Wagener, T., Goldscheider, N., 2018. Dynamics of water fluxes and storages in an Alpine karst catchment under current and potential future climate conditions. Hydrol. Earth Syst. Sci. 22, 3807–3823. https://doi.org/10.5194/hess-22-3807-2018.

Cheng, J., Lee, X., Theng, B.K.G., Zhang, L., Fang, B., Li, F., 2015. Biomass accumulation and carbon sequestration in an age-sequence of Zanthoxylum bungeanum plantations under the Grain for Green Program in karst regions, Guizhou province. Agr. Forest Meteorol. 203, 88–95. https://doi.org/10.1016/j.agrformet.2015.01.004.

Chiocchini, U., Castaldi, F., 2011. The impact of groundwater on the excavation of tunnels in two different hydrogeological settings in central ItalyL'impact des eaux souterraines sur le creusement de tunnels dans deux contextes hydrogéologiques différents en Italie centraleEl impacto del agua subterránea en la excavación de túneles en dos diferentes configuraciones hidrogeológicas en Italia central地下水对意大利中部两种不同水文地质条件下的隧道挖掘的影响O impacte da água subterrânea na escavação de túneis em dois ambientes hidrogeológicos distintos na Itália central. Hydrgeol. J. 19 (3), 651–669.

Cohen, W.B., Yang, Z., Stehman, S.V., Schroeder, T.A., Bell, D.M., Masek, J.G., Huang, C., Meigs, G.W., 2016. Forest disturbance across the conterminous United States from 1985–2012: The emerging dominance of forest decline. For. Ecol. Manage. 360, 242–252. https://doi.org/10.1016/j.foreco.2015.10.042.

Creutzfeldt, B., Heinrich, I., Merz, B., 2015. Total water storage dynamics derived from tree-ring records and terrestrial gravity observations. J. Hydrol. 529, 640–649. https://doi.org/10.1016/j.jhydrol.2015.04.006.

Degerli, B., Cetin, M., 2022. Evaluation from Rural to Urban Scale for the Effect of NDVI-NDBI Indices on Land Surface Temperature, in Samsun, Türkiye. Turkish JAF Sci. Tech. 10, 2446–2452. https://doi.org/10.24925/turjaf.v10i12.2446-2452.5535.

Degerli, B., Çetin, M., 2022. Using the Remote Sensing Method to Simulate the Land Change in the Year 2030. Turkish JAF Sci. Tech. 10, 2453–2466. https://doi.org/10.24925/turjaf.v10i12.2453-2466.5555.

Ding, Y., Nie, Y., Chen, H., Wang, K., Querejeta, J.I., 2021. Water uptake depth is coordinated with leaf water potential, water-use efficiency and drought vulnerability in karst vegetation. New Phytol. 229, 1339–1353. https://doi.org/10.1111/nph.16971.

Duchesne, L., Ouimet, R., Morneau, C., 2003. Assessment of sugar maple health based on basal area growth pattern. Can. J. For. Res. 33, 2074–2080. https://doi.org/10.1139/x03-141.

Eilmann, B., Rigling, A., 2012. Tree-growth analyses to estimate tree species' drought tolerance. Tree Physiol. 32, 178–187. https://doi.org/10.1093/treephys/tps004.

Eimil-Fraga, C., Rodríguez-Soalleiro, R., Sánchez-Rodríguez, F., Pérez-Cruzado, C., Álvarez-Rodríguez, E., 2014. Significance of bedrock as a site factordetermining nutritional status and growth of maritime pine. For. Ecol. Manage. 331, 19–24. https://doi.org/10.1016/j.foreco.2014.07.024.

Esper, J., Cook, E.R., Schweingruber, F.H., 2002. Low-frequency signals in long tree-ring chronologies for reconstructing past temperature variability. Sci. New Ser. 295 (5563), 2250–2253.

Estrada-Medina, H., Graham, R.C., Allen, M.F., Jiménez-Osornio, J.J., Robles-Casolco, S., 2013. The importance of limestone bedrock and dissolution karst features on tree root distribution in northern Yucatán, México. Plant Soil 362, 37–50. https://doi.org/10.1007/s11104-012-1175-x.

Fekedulegn, D., Hicks, R.R., Colbert, J.J., 2003. Influence of topographic aspect, precipitation and drought on radial growth of four major tree species in an Appalachian watershed. For. Ecol. Manage. 177 (1-3), 409–425.

Ferguson, G., George, S.S., 2003. historical and estimated ground water levels near Winnipeg, Canada, and their sensitivity to climatic variability. J. Am. Water Resour. Assoc. 39, 1249–1259. https://doi.org/10.1111/j.1752-1688.2003.tb03706.x.

Frank, D.C., Poulter, B., Saurer, M., Esper, J., Huntingford, C., Helle, G., Treydte, K., Zimmermann, N.E., Schleser, G.H., Ahlström, A., Ciais, P., Friedlingstein, P., Levis, S., Lomas, M., Sitch, S., Viovy, N., Andreu-Hayles, L., Bednarz, Z., Berninger, F., Boettger, T., D'Alessandro, C.M., Daux, V., Filot, M., Grabner, M., Gutierrez, E., Haupt, M., Hilasvuori, E., Jungner, H., Kalela-Brundin, M., Krapiec, M., Leuenberger, M., Loader, N.J., Marah, H., Masson-Delmotte, V., Pazdur, A., Pawelczyk, S., Pierre, M., Planells, O., Pukiene, R., Reynolds-Henne, C.E., Rinne, K. T., Saracino, A., Sonninen, E., Stievenard, M., Switsur, V.R., Szczepanek, M., Szychowska-Krapiec, E., Todaro, L., Waterhouse, J.S., Weigl, M., 2015. Water-use efficiency and transpiration across European forests during the Anthropocene. Nat. Clim. Change 5 (6), 579–583.

Gazol, A., Camarero, J.J., Sánchez-Salguero, R., Vicente-Serrano, S.M., Serra-Maluquer, X., Gutiérrez, E., Luis, M., Sangüesa-Barreda, G., Novak, K., Rozas, V., Tíscar, P.A., Linares, J.C., Martínez del Castillo, E., Ribas, M., García-González, I., Silla, F., Camisón, Á., Génova, M., Olano, J.M., Hereş, A.-M., Curiel Yuste, J., Longares, L.A., Hevia, A., Tomas-Burguera, M., Galván, J.D., Battipaglia, G., 2020. Drought legacies are short, prevail in dry conifer forests and depend on growth variability. J. Ecol. 108 (6), 2473–2484.

Gisbert, J., Vallejos, A., González, A., Pulido-Bosch, A., 2009. Environmental and hydrogeological problems in karstic terrains crossed by tunnels: a case study. Environ. Geol. 58, 347–357. https://doi.org/10.1007/s00254-008-1609-1.

Goldscheider, N., 2019. A holistic approach to groundwater protection and ecosystem services in karst terrains. Carbonates Evaporites 34, 1241–1249. https://doi.org/10.1007/s13146-019-00492-5.

Hasselquist, N.J., Allen, M.F., Santiago, L.S., 2010. Water relations of evergreen and drought-deciduous trees along a seasonally dry tropical forest chronosequence. Oecologia 164, 881–890. https://doi.org/10.1007/s00442-010-1725-y.
Heilman, J.L., McInnes, K.J., Kjelgaard, J.F., Keith Owens, M., Schwinning, S., 2009. Energy balance and water use in a subtropical karst woodland on the Edwards Plateau, Texas. J. Hydrol. 373, 426–435. https://doi.org/10.1016/j.jhydrol.2009.05.007.
Heilman, J.L., Litvak, M.E., McInnes, K.J., Kjelgaard, J.F., Kamps, R.H., Schwinning, S., 2014. Water-storage capacity controls energy partitioning and water use in karst ecosystems on the Edwards Plateau, Texas: water-storage controls water use in karst ecosystems. Ecohydrology 7, 127–138. https://doi.org/10.1002/eco.1327.
Jiang, Z., Lian, Y., Qin, X., 2014. Rocky desertification in Southwest China: Impacts, causes, and restoration. Earth Sci. Rev. 132, 1–12. https://doi.org/10.1016/j.earscirev.2014.01.005.
Jump, A.S., Hunt, J.M., Peñuelas, J., 2006. Rapid climate change-related growth decline at the southern range edge of *Fagus sylvatica*: *FAGUS* growth decline. Glob. Chang. Biol. 12, 2163–2174. https://doi.org/10.1111/j.1365-2486.2006.01250.x.
LeBlanc, D.C., Nicholas, N.S., Zedaker, S.M., 1992. Prevalence of individual-tree growth decline in red spruce populations of the southern Appalachian Mountains. Can. J. Forest Res. 22, 905–914. https://doi.org/10.1139/x92-120.
Lévesque, M., Saurer, M., Siegwolf, R., Eilmann, B., Brang, P., Bugmann, H., Rigling, A., 2013. Drought response of five conifer species under contrasting water availability suggests high vulnerability of Norway spruce and European larch. Glob. Chang. Biol. 19, 3184–3199. https://doi.org/10.1111/gcb.12268.
Li, J., Gou, X., Cook, E.R., Chen, F., 2006. Tree-ring based drought reconstruction for the central Tien Shan area in northwest China. Geophys. Res. Lett. 33, L07715. https://doi.org/10.1029/2006GL025803.
Li, J., Wang, Z., Lai, C., Wu, X., Zeng, Z., Chen, X., Lian, Y., 2018. Response of net primary production to land use and land cover change in mainland China since the late 1980s. Sci. Total Environ. 639, 237–247. https://doi.org/10.1016/j.scitotenv.2018.05.155.
Li, J., Hong, A., Yuan, D., Jiang, Y., Deng, S., Cao, C., Liu, J., 2021. A new distributed karst-tunnel hydrological model and tunnel hydrological effect simulations, 125639 J. Hydrol. 593. https://doi.org/10.1016/j.jhydrol.2020.125639.
Liu, Z., Li, K., Xiong, K., Li, Y., Wang, J., Sun, J., Cai, L., 2021b. Effects of Zanthoxylum bungeanum planting on soil hydraulic properties and soil moisture in a karst area, 107125 Agr. Water Manage. 257. https://doi.org/10.1016/j.agwat.2021.107125.
Liu, F., Liu, H., Xu, C., Shi, L., Zhu, X., Qi, Y., He, W., 2021a. Old-growth forests show low canopy resilience to droughts at the southern edge of the taiga. Glob. Chang. Biol. 27, 2392–2402. https://doi.org/10.1111/gcb.15605.
Liu, L., Peng, J., Li, G., Guan, J., Han, W., Ju, X., Zheng, J., 2023. Effects of drought and climate factors on vegetation dynamics in Central Asia from 1982 to 2020, 116997 J. Environmen. Manage. 328. https://doi.org/10.1016/j.jenvman.2022.116997.
Liu, J., Shen, L., Wang, Z., Duan, S., Wu, W., Peng, X., Wu, C., Jiang, Y., 2019. Response of plants water uptake patterns to tunnels excavation based on stable isotopes in a karst trough valley. J. Hydrol. 571, 485–493. https://doi.org/10.1016/j.jhydrol.2019.01.073.
Lu, Z.-X., Wang, P., Ou, H.-B., Wei, S.-X., Wu, L.-C., Jiang, Y., Wang, R.-J., Liu, X.-S., Wang, Z.-H., Chen, L.-J., Liu, Z.-M., 2022. Effects of different vegetation restoration on soil nutrients, enzyme activities, and microbial communities in degraded karst landscapes in southwest China, 120002 For. Ecol. Manage. 508. https://doi.org/10.1016/j.foreco.2021.120002.
Lv, Y., Jiang, Y., Hu, W., Cao, M., Mao, Y., 2020. A review of the effects of tunnel excavation on the hydrology, ecology, and environment in karst areas: current status, challenges, and perspectives, 124891 J. Hydrol. 586. https://doi.org/10.1016/j.jhydrol.2020.124891.
Lv, Y., Jiang, J., Chen, L., Hu, W., Jiang, Y., 2022. Elaborate simulation and predication of the tunnel drainage effect on karst groundwater field and discharge based on Visual MODFLOW, 128023 J. Hydrol. 612. https://doi.org/10.1016/j.jhydrol.2022.128023.
McCole, A.A., Stern, L.A., 2007. Seasonal water use patterns of Juniperus ashei on the Edwards Plateau, Texas, based on stable isotopes in water. J. Hydrol. 342, 238–248. https://doi.org/10.1016/j.jhydrol.2007.05.024.
McDowell, N.G., Beerling, D.J., Breshears, D.D., Fisher, R.A., Raffa, K.F., Stitt, M., 2011. The interdependence of mechanisms underlying climate-driven vegetation mortality. Trends Ecol. Evol. 26, 523–532. https://doi.org/10.1016/j.tree.2011.06.003.
Muzika, R.M., Guyette, R.P., Zielonka, T., Liebhold, A.M., 2004. The influence of O3, NO2 and SO2 on growth of Picea abies and Fagus sylvatica in the Carpathian Mountains. Environ. Pollut. 130, 65–71. https://doi.org/10.1016/j.envpol.2003.10.021.
Nie, Y., Chen, H., Wang, K., Tan, W., Deng, P., Yang, J., 2011. Seasonal water use patterns of woody species growing on the continuous dolostone outcrops and nearby thin soils in subtropical China. Plant Soil 341, 399–412. https://doi.org/10.1007/s11104-010-0653-2.
Obojes, N., Meurer, A., Newesely, C., Tasser, E., Oberhuber, W., Mayr, S., Tappeiner, U., 2018. Water stress limits transpiration and growth of European larch up to the lower subalpine belt in an inner-alpine dry valley. New Phytol. 220, 460–475.
Parise, M., Gunn, J., 2007. Natural and anthropogenic hazards in karst areas: an introduction. In: Natural and Anthropogenic Hazards in Karst Areas: Recognition, Analysis and Mitigation. Geological Society of London, London, pp. 1.
Park Williams, A., Allen, C.D., Macalady, A.K., Griffin, D., Woodhouse, C.A., Meko, D.M., Swetnam, T.W., Rauscher, S.A., Seager, R., Grissino-Mayer, H.D., Dean, J.S., Cook, E.R., Gangodagamage, C., Cai, M., McDowell, N.G., 2013. Temperature as a potent driver of regional forest drought stress and tree mortality. Nat. Clim. Change 3, 292–297. https://doi.org/10.1038/nclimate1693.
Peng, T., Wang, S., 2012. Effects of land use, land cover and rainfall regimes on the surface runoff and soil loss on karst slopes in southwest China. Catena 90, 53–62. https://doi.org/10.1016/j.catena.2011.11.001.
Peñuelas, J., Hunt, J.M., Ogaya, R., Jump, A.S., 2008. Twentieth century changes of tree-ring $\delta^{13}C$ at the southern range-edge of *Fagus sylvatica:* increasing water-use efficiency does not avoid the growth decline induced by warming at low altitudes: BEECH $\delta^{13}C$ under growth decline. Glob. Chang. Biol. 14, 1076–1088. https://doi.org/10.1111/j.1365-2486.2008.01563.x.
Pesendorfer, M., Loew, S., 2010. Subsurface exploration and transient pressure testing from a deep tunnel in fractured and karstified limestones (Lötschberg Base Tunnel, Switzerland). IInt. J. Rock Mech. Min. 47, 121–137. https://doi.org/10.1016/j.ijrmms.2009.09.013.
Phillips, O.L., van der Heijden, G., Lewis, S.L., López-González, G., Aragão, L.E.O.C., Lloyd, J., Malhi, Y., Monteagudo, A., Almeida, S., Dávila, E.A., Amaral, I., Andelman, S., Andrade, A., Arroyo, L., Aymard, G., Baker, T.R., Blanc, L., Bonal, D., de Oliveira, Á.C.A., Chao, K.-J., Cardozo, N.D., da Costa, L., Feldpausch, T.R., Fisher, J.B., Fyllas, N.M., Freitas, M.A., Galbraith, D., Gloor, E., Higuchi, N., Honorio, E., Jiménez, E., Keeling, H., Killeen, T.J., Lovett, J.C., Meir, P., Mendoza, C., Morel, A., Vargas, P.N., Patiño, S., Peh, K.-H., Cruz, A.P., Prieto, A., Quesada, C.A., Ramírez, F., Ramírez, H., Rudas, A., Salamão, R., Schwarz, M., Silva, J., Silveira, M., Ferry Slik, J.W., Sonké, B., Thomas, A.S., Stropp, J., Taplin, J.R.D., Vásquez, R., Vilanova, E., 2010. Drought-mortality relationships for tropical forests. New Phytol. 187 (3), 631–646.
Phipps, R.L., Whiton, J.C., 1988. Decline in long-term growth trends of white oak. Can. J. Forest Res. 18, 24–32. https://doi.org/10.1139/x88-005.
Piao, S., Mohammat, A., Fang, J., Cai, Q., Feng, J., 2006. NDVI-based increase in growth of temperate grasslands and its responses to climate changes in China. Glob. Environ. Chang. 16, 340–348. https://doi.org/10.1016/j.gloenvcha.2006.02.002.
Potter, C.S., Randerson, J.T., Field, C.B., Matson, P.A., Vitousek, P.M., Mooney, H.A., Klooster, S.A., 1993. Terrestrial ecosystem production: a process model based on global satellite and surface data. Glob. Biogeochem. Cy. 7, 811–841. https://doi.org/10.1029/93GB02725.
Querejeta, J.I., Estrada-Medina, H., Allen, M.F., Jiménez-Osornio, J.J., 2007. Water source partitioning among trees growing on shallow karst soils in a seasonally dry tropical climate. Oecologia 152, 26–36. https://doi.org/10.1007/s00442-006-0629-3.
Raynolds, M., Comiso, J., Walker, D., Verbyla, D., 2008. Relationship between satellite-derived land surface temperatures, arctic vegetation types, and NDVI. Remote Sens. Environ. 112, 1884–1894. https://doi.org/10.1016/j.rse.2007.09.008.
Rong, L., Chen, X.i., Chen, X., Wang, S., Du, X., 2011. Isotopic analysis of water sources of mountainous plant uptake in a karst plateau of southwest China. Hydrol. Process. 25, 3666–3675. https://doi.org/10.1002/hyp.8093.
Ryel, R.J., Leffler, A.J., Ivans, C., Peek, M.S., Caldwell, M.M., 2010. Functional differences in water-use patterns of contrasting life forms in great basin steppelands. Vadose Zone J. 9, 548–560. https://doi.org/10.2136/vzj2010.0022.
Sahin, G., Cabuk, S.N., Cetin, M., 2022. The change detection in coastal settlements using image processing techniques: a case study of Korfez. Environ. Sci. Pollut. Res. 29, 15172–15187. https://doi.org/10.1007/s11356-021-16660-x.
Schuster, R., Oberhuber, W., 2013. Drought sensitivity of three co-occurring conifers within a dry inner Alpine environment. Trees 27, 61–69. https://doi.org/10.1007/s00468-012-0768-6.
Schwinning, S., 2010. The ecohydrology of roots in rocks. Ecohydrology 3, 238–245. https://doi.org/10.1002/eco.134.
Seddon, A.W.R., Macias-Fauria, M., Long, P.R., Benz, D., Willis, K.J., 2016. Sensitivity of global terrestrial ecosystems to climate variability. Nature 531, 229–232. https://doi.org/10.1038/nature16986.
Seidl, R., Schelhaas, M.-J., Rammer, W., Verkerk, P.J., 2014. Increasing forest disturbances in Europe and their impact on carbon storage. Nat. Clim. Change 4, 806–810. https://doi.org/10.1038/nclimate2318.
Stokes, M.A., Smiley, T.L., 1996. An Introduction to Tree-ring Dating. University of Arizona Press.
Suratman, M.N. (Ed.), 2022. Concepts and Applications of Remote Sensing in Forestry. Springer Nature Singapore, Singapore.
Tong, X., Brandt, M., Yue, Y., Horion, S., Wang, K., Keersmaecker, W.D., Tian, F., Schurgers, G., Xiao, X., Luo, Y., Chen, C., Myneni, R., Shi, Z., Chen, H., Fensholt, R., 2018. Increased vegetation growth and carbon stock in China karst via ecological engineering. Nat. Sustain. 1, 44–50. https://doi.org/10.1038/s41893-017-0004-x.
Vicente-Serrano, S.M., Camarero, J.J., Olano, J.M., Martín-Hernández, N., Peña-Gallardo, M., Tomás-Burguera, M., Gazol, A., Azorin-Molina, C., Bhuyan, U., El Kenawy, A., 2016. Diverse relationships between forest growth and the Normalized Difference Vegetation Index at a global scale. Remote Sens. Environ. 187, 14–29. https://doi.org/10.1016/j.rse.2016.10.001.
Vincenzi, V., Gargini, A., Goldscheider, N., 2009. Using tracer tests and hydrological observations to evaluate effects of tunnel drainage on groundwater and surface waters in the Northern Apennines (Italy)Utilisation de tests de traçage et d'observations hydrologiques dans le but d'évaluer les conséquence du drainage d'un tunnel sur les eaux souterraines et sur les eaux de surface dans le Nord des Apennins (Italie)Markierungsversuche und hydrologische Beobachtungen zur Bewertung der Auswirkungen von Tunneldrainage auf Grund- und Oberflächenwässer im nördlichen Apennin (Italien)Uso de ensayos de trazadores y observaciones hidrológicas en la evaluación de los efectos del drenaje de un túnel sobre las aguas subterráneas y superficiales en los Apeninos del Norte (Italia)应用示踪试验和水文观测评估意大利亚平宁北部某隧道排水对地下水和地表水的影响Prove di tracciamento e misure idrologiche per valutare gli effetti del drenaggio di una galleria sulle acque sotterranee e superficiali nell'Appennino Settentrionale (Italia) Utilização de traçadores e dados hidrológicos para avaliação de efeitos da drenagem

de túneis em águas subterrâneas e superficiais no Norte dos Apeninos (Itália). Hydrgeol. J. 17 (1), 135–150.
Wang, S., Ji, H., Ouyang, Z., Zhou, D., Zhen, L., Li, T., 1999. Preliminary study on weathering and pedogenesis of carbonate rock. Sci. China Ser. D-Earth Sci. 42, 572–581. https://doi.org/10.1007/BF02877784.
Wang, S., Liu, Q., Zhang, D., 2004. Karst rocky desertification in southwestern China: geomorphology, land use, impact and rehabilitation. Land Degrad. Dev. 15, 115–121. https://doi.org/10.1002/ldr.592.
Wang, K., Zhang, C., Chen, H., Yue, Y., Zhang, W., Zhang, M., Qi, X., Fu, Z., 2019. Karst landscapes of China: patterns, ecosystem processes and services. Landsc. Ecol. 34, 2743–2763. https://doi.org/10.1007/s10980-019-00912-w.
Wilmking, M., Maaten-Theunissen, M., Maaten, E., Scharnweber, T., Buras, A., Biermann, C., Gurskaya, M., Hallinger, M., Lange, J., Shetti, R., Smiljanic, M., Trouillier, M., 2020. Global assessment of relationships between climate and tree growth. Glob. Chang. Biol. 26, 3212–3220. https://doi.org/10.1111/gcb.15057.
Xiao, H., Weng, Q., 2007. The impact of land use and land cover changes on land surface temperature in a karst area of China. J. Environ. Manage. 85, 245–257. https://doi.org/10.1016/j.jenvman.2006.07.016.
Xu, P., Fang, W., Zhou, T., Zhao, X., Luo, H., Hendrey, G., Yi, C., 2019. Spatial upscaling of tree-ring-based forest response to drought with satellite data. Remote Sens-Basal. 11, 2344. https://doi.org/10.3390/rs11202344.
Yan, Y., Dai, Q., Hu, G., Jiao, Q., Mei, L., Fu, W., 2020. Effects of vegetation type on the microbial characteristics of the fissure soil-plant systems in karst rocky desertification regions of SW China, 136543 Sci. Total Environ. 712. https://doi.org/10.1016/j.scitotenv.2020.136543.
Yang, J., Nie, Y., Chen, H., Wang, S., Wang, K., 2016. Hydraulic properties of karst fractures filled with soils and regolith materials: Implication for their ecohydrological functions. Geoderma 276, 93–101. https://doi.org/10.1016/j.geoderma.2016.04.024.
Zhang, X., Bai, X., He, X., 2011. Soil creeping in the weathering crust of carbonate rocks and underground soil losses in the karst mountain areas of southwest china. Carbonates Evaporites 26, 149–153. https://doi.org/10.1007/s13146-011-0043-8.
Zhao, M., Running, S.W., 2010. Drought-induced reduction in global terrestrial net primary production from 2000 through 2009. Science 329, 940–943. https://doi.org/10.1126/science.1192666.
Zheng, W., Wang, X., Tang, Y., Liu, H., Wang, M., Zhang, L., 2017. Use of tree rings as indicator for groundwater level drawdown caused by tunnel excavation in Zhongliang Mountains, Chongqing, Southwest China. Environ. Earth Sci. 76, 522. https://doi.org/10.1007/s12665-017-6859-3.
Zheng, X., Yang, Z., Wang, S., Chen, Y.-F., Hu, R., Zhao, X.-J., Wu, X.-L., Yang, X.-L., 2021. Evaluation of hydrogeological impact of tunnel engineering in a karst aquifer by coupled discrete-continuum numerical simulations, 125765 J. Hydrol. 597. https://doi.org/10.1016/j.jhydrol.2020.125765.
Zweifel, R., Zimmermann, L., Zeugin, F., Newbery, D.M., 2006. Intra-annual radial growth and water relations of trees: implications towards a growth mechanism. J. Exp. Bot. 57, 1445–1459. https://doi.org/10.1093/jxb/erj125.